Swapping carbonate for silicate in agricultural enhanced rock weathering

Tyler Kukla[1], Yoshiki Kanzaki[2], Freya Chay[1], Noah J. Planavsky[3,4], Christopher T. Reinhard[2]

[1]CarbonPlan, San Francisco, CA, USA
[2]School of Earth and Atmospheric Sciences, Georgia Institute of Technology, Atlanta, GA, USA
[3]Department of Earth and Planetary Sciences, Yale University, New Haven, CT, USA
[4]Yale Center for Natural Carbon Capture, New Haven, CT, USA

Key Points:

- Calcite and basalt can both be effective feedstocks for carbon removal.
- Basalt weathering is more responsive to changes in the amount and fineness of rock than calcite.
- Calcite and basalt carbon removal trade-offs depend on carbon accounting decisions including the system boundaries in space and time.

Corresponding author: Tyler Kukla, tyler@carbonplan.org

Abstract

Enhanced rock weathering with crushed silicates is often considered as an alternative to agricultural liming for soil pH management and carbon dioxide removal. But swapping carbonates for silicates does not guarantee better carbon removal outcomes. Carbonates weather rapidly, and recent work has found that they can remove more carbon than fast-reacting silicates in some environments. On the other hand, carbonate dissolution can mobilize fossil carbon and potentially lead to carbon emissions, depending on the spatial and temporal boundaries of the system. Here, we use a one-dimensional reactive transport model, SCEPTER, to analyze the conditions where carbonate weathering breaks even with basalt — a common silicate rock used in enhanced weathering — from an end-to-end carbon removal perspective. We show that current liming practices can remove more carbon than basalt enhanced weathering projects, especially in less acidic conditions and at lower rock application fluxes. However, the methods for increasing silicate weathering carbon removal — including adding more and finer rock — are generally less effective for carbonates. We also show how the carbonate-silicate break-even line changes when we consider the effects of downstream losses, upstream emissions, and carbon accounting decisions. Our results emphasize how existing agricultural practices can be optimized for carbon removal, and present a series of key questions that will be critical for attempts to navigate the carbonate-silicate swap on managed lands.

Plain Language Summary

Enhanced weathering is a carbon removal strategy that often involves spreading crushed rock on agricultural fields. It is a promising carbon removal strategy in part because spreading rocks on fields is not new — farmers have been "liming" for generations to add nutrients to the soil and reduce its acidity. While enhanced weathering is commonly done with silicate rocks, liming is often done with carbonates. Both types of rock are capable of carbon removal, but they differ in important ways. As the name implies, carbonates have carbon in them, which limits how much carbon they can remove from the atmosphere. But carbonates also tend to dissolve quickly, which can increase carbon removal. We used a model to explore these trade-offs and better understand which rocks to spread where for carbon removal. We found that, compared to basalt, carbon removal with carbonates is much less sensitive to how much rock is spread and how finely it is crushed. We also show that the perceived climate impact of spreading rocks can depend on the equation used to calculate carbon removal. Our analysis presents a framework that is useful for navigating which rocks to spread to achieve good outcomes for the climate.

1 Introduction

Silicate-based enhanced weathering has become a focal point of carbon dioxide removal (CDR) research and policy, in part because it promises both climate and agronomic benefits. When silicate rocks weather in agricultural fields, they can introduce nutrients, raise soil pH, and facilitate carbon removal (Baek et al., 2023; Beerling et al., 2024; Buckingham & Henderson, 2024; Haque et al., 2020; Hartmann et al., 2013; Vienne et al., 2022). However, it is not often acknowledged that a version of enhanced rock weathering is already widely practiced. Farmers in many parts of the world apply carbonate rock dust — commonly known as aglime — to manage soil pH. Depending on local conditions and the timescale considered, carbonate rocks can act as a source or sink of CO_2 when they dissolve, raising questions about where to spread carbonates for carbon removal and where to swap them for silicates instead. To effectively advance enhanced weathering, we need a clearer understanding of the trade-offs between carbonate and silicate applications in agricultural systems.

Carbonates and silicates exhibit a core geochemical trade-off: carbonates tend to weather more quickly and completely (Dreybrodt, 1988; Dreybrodt et al., 1996) — but remove less carbon per unit of alkalinity released. This is because carbonates, such as calcite ($CaCO_3$), contain fossil carbon in their mineral structure, which limits the amount of atmospheric CO_2 the weathering reaction can consume. While carbonate weathering can act as a carbon sink in many contexts (Gaillardet et al., 1999, 2019; Hamilton et al., 2007; Oh & Raymond, 2006), it can also become a source if that fossil carbon makes its way into the atmosphere (Lerman & Wu, 2006; Perrin et al., 2008; Zamanian et al., 2021). This means that downstream losses — reactions that reverse the CDR achieved by rock weathering — are especially consequential for carbonate CDR, since they can tip the system from a carbon sink into a source. In contrast, silicate minerals do not contain fossil carbon. While silicate weathering reactions generally proceed more slowly, they will never directly emit new carbon to the atmosphere and they offer greater carbon removal per unit of alkalinity released.

Whether liming is a carbon source or sink depends, in part, on the spatial and temporal scope of the carbon fluxes in question. Limestone weathering might emit carbon locally (Dietzen et al., 2018; Perrin et al., 2008; Zamanian et al., 2021), but remove it at the catchment scale by preventing acid-driven degassing downstream (Raymond et al., in press). Similarly, cation sorption in soils can cause limestone weathering to be an immediate carbon source and a sink later when the sorption is reversed (Kanzaki et al., 2025; Raymond et al., in press). Liming can also modify soil organic carbon fluxes, with the sign of change varying over space and time (Dietzen et al., 2018; Fornara et al., 2011; Grover et al., 2017; Wang et al., 2021; H.-M. Zhang et al., 2022).

When studies discuss the effect of swapping an existing liming practice for enhanced silicate weathering, however, some of this nuance can be lost. Liming is often treated as a carbon source (*e.g.,* West & McBride, 2005), and silicates presented as an opportunity to avoid liming emissions while also removing carbon (*e.g.,* Beerling et al., 2018, 2024, 2025; Dietzen et al., 2018). But there has long been evidence that liming can remove more carbon than it emits, even in systems that are not optimized for carbon removal (Hamilton et al., 2007; Oh & Raymond, 2006; S. Zhang et al., 2022). Moreover, tonne-for-tonne, carbonates often have a higher carbon removal potential than silicates. All else equal, that means sourcing carbonate rock requires fewer emissions per unit of potential removal.

Evidence from natural and agricultural systems indicates that carbonate amendments such as liming could remove as much or more carbon than silicate amendments. Due to its rapid dissolution kinetics, carbonate weathering in natural systems accounts for most (∼60%) of the global river alkalinity flux, despite making up less than 20% of terrestrial bedrock (Gaillardet et al., 1999, 2019; Moon et al., 2014). In agricultural fields, rapid weathering rates allow carbonate liming to achieve the same soil pH increases in a matter of months that silicate amendments might take years to achieve (Beerling et al., 2024; Jones & Mallarino, 2018; Pagani & Mallarino, 2012). Recent enhanced weathering work has shown that carbonates can remove more carbon than even fast-reacting silicate minerals like dunite in certain environments (Fuhr et al., 2025). Still, carbonate weathering rates are not universally high. Carbonate can saturate in soils relatively easily, at which point it is more likely to precipitate than dissolve. Silicates, on the other hand, may be less saturation-limited, making them more effective in neutral-to-alkaline soils and at high rock application fluxes (Schuiling et al., 2011; Suarez & Rhoades, 1982). Overall, it is clear that it is inappropriate to assume liming is always a source of emissions, and that comparing the carbon removal effects of enhanced carbonate and silicate weathering requires more nuance.

Here, we simulate the carbonate-silicate trade-off dynamics in an idealized system. Our analysis focuses on the carbon removal break-even line, defined by the quantity and fineness of a silicate feedstock that produces the same carbon removal outcome as a baseline carbonate amendment. We simulate amendments of calcite, a common liming agent,

and basalt, a common enhanced weathering feedstock, in conditions similar to the U.S. Great Plains Corn Belt — a region where liming is practiced extensively and long-term basalt enhanced rock weathering field trials are already underway (Kantola et al., 2023; Beerling et al., 2024). We explore how the break-even line changes when we account for downstream losses and upstream emissions, and how the carbon accounting rules used to quantify carbon removal can change our perception of the trade-offs involved in swapping conventional aglime for silicate feedstocks.

2 Methods

Our analysis leverages SCEPTER v1.01 to simulate field-scale carbon fluxes in response to carbonate and silicate amendments (Kanzaki et al., 2024) (Code at `https://github.com/cdr-laboratory/SCEPTER/releases/tag/v1.0.1`). We pair these simulations with an emissions model to estimate the emissions associated with crushing and transporting the feedstock to the field. We also apply multiple carbon accounting approaches to calculate net CDR and compare the performance of calcite versus basalt weathering.

2.1 SCEPTER modeling

All SCEPTER simulations are run from the same 10,000 year spin-up simulation that was tuned to match soil conditions consistent with the Great Plains of the U.S. Following Kanzaki et al. (2025), we use four tuning parameters: (1) the surface dissolved Ca^{2+} concentration, a proxy for historical liming and background carbonate weathering; (2) an aggregate cation exchange coefficient; (3) the flux of organic carbon into the soil; and (4) the turnover time of soil organic carbon. These parameters are tuned to match data for soil pH, base saturation, organic matter content, and soil pCO_2 (Table S1 in Supporting Information).

All simulations are run with a 0.5m deep soil column discretized to 30 grid cells and adopt the boundary conditions from site 311 of Kanzaki et al. (2025). Mean annual temperature is set to 8.2 ^{o}C, the net water infiltration rate is 0.35 m yr^{-1}, the mixing depth for organic matter is 0.25m, the initial porosity is 0.45 (unitless), and the initial water saturation at the surface is 0.63 (unitless). We tune the model with cation exchange processes turned on for consistency with Kanzaki et al. (2025), but we turn off cation exchange in our rock amendment simulations in order to isolate the impacts of feedstock dissolution on the carbonate-silicate swap. Cation exchange reactions can introduce lags between alkalinity release and carbon removal (or alkalinity consumption), and these lags are highly sensitive to the initial soil conditions and liming history (Kanzaki et al., 2025). We demonstrate how cation exchange processes can affect carbon removal outcomes in the supporting information (Supporting Information Fig. S1), though a more detailed analysis of cation exchange impacts is left for future work.

2.1.1 Soil pH variation

In order to compare the results from less and more acidic soils that are otherwise identical, we vary soil acidity by applying ammonium nitrate fertilizer at different rates. In our less acidic system, we apply 0.03 t ha^{-1} of fertilizer annually ($\sim$ 1 gN m^{-2} yr^{-1}) and, in our more acidic system, we apply $\sim$ 0.35 t ha^{-1} annually ($\sim$ 12.3 gN m^{-2} yr^{-1}). These values roughly capture the range of fertilizer application across the Corn Belt today (Cao et al., 2018; Lu & Tian, 2017; Nishina et al., 2017). Ammonium from fertilizer (or natural sources such as the mineralization of organic N) can generate acidity by nitrification following

$$NH_4^+ + 2O_2 \rightarrow NO_3^- + H_2O + 2H^+. \quad (1)$$

The extent of nitrification and denitrification determine the net production of anthropogenic strong (non-carbonic) acid in the soil which, in turn, acts to govern whether calcite is an immediate carbon source or sink as it weathers in the field. Calcite weathering by nitric acid releases CO_2 by

$$CaCO_3 + 2HNO_3 \rightarrow Ca^{2+} + 2NO_3^- + CO_2 + H_2O. \quad (2)$$

However, weathering by carbonic acid removes CO_2. Carbonic acid can be assumed to be in equilibrium with the soil-atmosphere system such that

$$CO_2 + H_2O \rightleftharpoons H_2CO_3, \quad (3)$$

and calcite dissolution by carbonic acid can be written as

$$CaCO_3 + H_2CO_3 \rightarrow Ca^{2+} + 2HCO_3^-. \quad (4)$$

Carbonic acid weathering effectively shifts equation 3 to the right, taking up CO_2. While the stoichiometry is different, the effect of non-carbonic acid weathering on silicates is similar — carbonic acid neutralization results in the direct uptake of CO_2 in the field whereas non-carbonic acid neutralization does not.

2.1.2 Feedstock variation

Our simulations explore two key variables that could be optimized for carbon removal in an ideal deployment — the amount and size of rock dust applied. Starting from the same spin-up, each simulation applies rock and fertilizer at a uniform rate for 0.05 years ($\sim$ 2.5 weeks) at the start of each year for 15 years. We use an annual cadence because it is common in the enhanced weathering literature, though we note that traditional liming cadences can be longer ($\sim 3-5$ years). Rock application rates range from 0.1-60 tonnes ha^{-1} yr^{-1} and the mean dust particle diameter varies from 2-600 μm. Each particle size distribution is defined as a narrow Gaussian with a standard deviation of ~ 1 μm. Particle diameter is related to the reactive surface area using a surface roughness formulation developed for basalt (*e.g.,* Kanzaki et al., 2022; Navarre-Sitchler & Brantley, 2007). With this formulation, the reactive surface area depends on the soil porosity, the mineral volume fraction, and the product of the geometric surface area (that of a sphere with the defined radius) and the roughness factor, which is also a function of the radius and evolves over time. Lacking an analog, we apply the same roughness formulation to calcite — a reasonable approximation given that carbon removal from calcite is relatively insensitive to the reactive surface area in the model.

To explore the sensitivity of the surface area parameterization, we repeat our simulations under two additional experimental conditions. First, we turn off explicit particle size tracking in the model. This requires parameterizing the relationship between the pore surface area and the effective radius of particles. The resulting reactive surface area depends on the roughness and the hydraulic radius of the pores in the soil column following equations 27, 29, and 39 in Kanzaki et al. (2022). Compared to particle size tracking, this parameterization tends to decrease basalt weathering fluxes, all else being equal. Second, we assume zero roughness (a roughness factor of one), so the geometric surface area is the reactive surface area, and we keep particle size tracking turned off. This set of simulations is not very realistic because crushing does not result in perfect spheres, but it is useful as a low-weatherability end-member for the rock amendment.

We simulate the same range of feedstock amount and particle diameter for both basalt and calcite amendments. However, to directly compare calcite and basalt outcomes we define a single baseline calcite practice that the basalt amendment replaces. Specifically, we set the particle diameter to 200 μm and the application flux to 1.0 ton ha^{-1} yr^{-1}. We chose this application flux because it yields some carbon removal in our less acidic case, and negligible removal in the more acidic case. Liming practices vary from

one site to another, but these values are within the range of liming recommendations across the Great Plains (Godsey et al., 2007; Jones & Mallarino, 2018; Lentz et al., 2010; Mallarino et al., 2023).

2.1.3 Carbon removal calculation

We compute carbon removal due to feedstock dissolution using carbon fluxes from the gas phase in the soil. We call the result of this calculation "initial CDR" (R) because it represents the amount of carbon removed locally before downstream effects and upstream emissions are considered.

The soil $p\mathrm{CO}_2$ mass balance in SCEPTER follows a general equation where the storage flux of the column (F_S) is balanced by inputs from the breakdown and dissolution of carbon-bearing organic (F_org) and inorganic (F_inorg) species and outputs from diffusion (F_dif) out of the top of the soil column and advection (F_adv) out of the bottom of the soil (see Text S1 in Supporting Information or Kanzaki et al. (2022) for more information on the general gas phase mass balance in SCEPTER). The resulting mass balance equation for soil $p\mathrm{CO}_2$ can be written as

$$F_\mathrm{S} = -F_\mathrm{org} - F_\mathrm{inorg} - F_\mathrm{dif} - F_\mathrm{adv}, \tag{5}$$

where all fluxes are in mol m^{-2} yr^{-1} and F_org and F_inorg represent the sum of all organic and inorganic species, respectively. Positive values indicate a flux out of the soil column.

To compute the initial CDR (R), we take the change in the diffusive flux at the top of the soil column compared to a control run where fertilizer is applied, but alkaline feedstock is not. We subtract out any decrease in the diffusive flux that could have been caused by decreased F_org (*i.e.,* respiration), giving us

$$R_X = -F_{\mathrm{dif},X,\mathrm{case}} + F_{\mathrm{dif},X,\mathrm{ctrl}} - \mathrm{MAX}\left(-F_{\mathrm{org},X,\mathrm{case}} + F_{\mathrm{org},X,\mathrm{ctrl}},\ 0\right) - F_{\mathrm{loss},X}, \tag{6}$$

where the subscript X is a stand-in for the feedstock, and the subscripts case and ctrl refer to a rock application run and the no-application control, respectively. F_loss is the flux of carbon re-emitted to the atmosphere downstream and is taken as a prescribed fraction of F_adv, consistent with Baek et al. (2023). Equation 6 works for both silicate and aglime feedstocks since F_dif includes any increase in CO_2 emissions caused by carbonate mineral dissolution via an increase in F_inorg.

To understand the sensitivity of R_X to model parameters other than the amount and fineness of rock, we conducted a sensitivity analysis using the Morris method as implemented in the SALib package in Python (see Text S2 and Table S2 in Supporting Information) (Campolongo et al., 2007; Herman & Usher, 2017; Iwanaga et al., 2022; Morris, 1991; Ruano et al., 2012). Results show that mean annual temperature and the soil water infiltration rate have large effects on R_calcite and R_basalt, and the difference between them (Fig. S2 in Supporting Information). Other deployment decisions, such as the depth of feedstock mixing and the duration of rock application, have relatively small effects in our model configuration.

By focusing on the carbon flux at the soil-atmosphere interface, R_X directly represents carbon removal from the atmosphere. However, this treatment ignores further-field effects on the carbon budget, such as the carbon emissions that are prevented by exporting less acid from the model domain. We also note that field quantification often derives removal from the flux of cations leached below some soil depth (usually the sampling depth). This flux corresponds with a "potential" CDR, which must be corrected for the carbon-removing component of weathering to derive the actual CDR (*e.g.,* Kanzaki et al., 2025; Reershemius et al., 2023). After this correction, the cation flux estimate is conceptually similar to quantifying CDR based on the F_adv term. We present the F_adv calculation and show that it is consistent with the analogous cation-driven CDR poten-

tial estimate in SCEPTER in the Supporting Information (Supporting Information Fig. S3).

2.2 Emissions model

We calculate emissions associated with crushing and transporting rock feedstock using the equations of B. Zhang et al. (2023). Their analysis focuses on the upper Midwest of the United States and presents emissions factors for different modes of transport and electrical grid regions (Table S3 in the Supporting Information). We use the electricity emissions factor they present for the Midwest Reliability Organization. We also adopt their Bond work index for basalt (18.67) and use this to compute the energy required for feedstock crushing. For calcite we assign a Bond work index of 12.10 — the mean limestone estimate of Kanda and Kotake (2007) and Bond (1961). Before crushing, we assume basalt and calcite have a sandy texture with particle diameters $\sim 1,300$ μm. Unless otherwise stated, we assume that crushed rock is transported to the field site via a 100 km truck trip. B. Zhang et al. (2023) found the emissions from spreading the rock to be negligible compared to crushing and transport, so we ignore them here.

While our emission model inputs are reasonable for the Corn Belt, it is hard to know if they are broadly representative. The emissions intensity of crushing can change by nearly a factor of three from state to state across the Great Plains, and the emissions factor estimated by B. Zhang et al. (2023) could be on the high end for the region (Li et al., 2024). There is also debate over a characteristic Bond work index for basalt, with recent estimates as high as ~ 30 (Li et al., 2024). Moreover, projects that use waste fines sieved down to the desired grain size may have no crushing emissions at all. These decisions impact our emissions fluxes, but they are generally less important than the amount and distance of rock transport (Fig. S4 in Supporting Information).

2.3 Carbon accounting

We adopt three basic accounting equations to compare the removals and emissions associated with basalt and calcite applications. In each equation, a positive removal indicates a carbon flux out of the atmosphere, and a positive emission is a carbon flux into the atmosphere. The equations treat removals and emissions differently, and therefore inform slightly different questions about the system. While they represent three possible lenses through which to view the silicate-carbonate trade-off, they are not an exhaustive list of accounting possibilities. For example, the spatial and temporal bounds used to simulate the initial removal flux represent a key accounting choice that could change the perception of the trade-offs between rock amendments, but we do not explore those here.

The first equation only considers the net removal flux (net R), ignoring upstream emissions. Here, net R is the difference between the initial removal due to the enhanced weathering project and that due to the baseline liming practice such that

$$\text{net R} = \text{R}_{\text{project}} - \text{R}_{\text{baseline}}. \tag{7}$$

Unless otherwise stated, the project refers to a basalt amendment and the baseline refers to the prescribed calcite amendment. This simplified equation is useful for understanding the geochemical effects on the climate outcomes. The second equation builds on equation 7 by incorporating the change in upstream emissions, E, where

$$\text{net R} - \text{E} = (\text{R}_{\text{project}} - \text{R}_{\text{baseline}}) - (\text{E}_{\text{project}} - \text{E}_{\text{baseline}}). \tag{8}$$

Finally, the third equation involves two modifications to equation 8, both of which help isolate the carbon removal flux from avoided emissions. The voluntary carbon market treats removals and avoided emissions as distinct climate benefits, recognizing that

they play different roles in reaching our climate goals (Nordahl et al., 2024). Avoided emissions could be conflated with removals if (1) $R_{baseline}$ is negative (*i.e.,* fossil carbon is emitted to the atmosphere); or (2) $E_{baseline}$ is greater than the portion of $E_{project}$ that replaces the baseline activity (Kukla et al., 2024). The first case is handled by requiring $R_{baseline}$ to be zero or positive. The second case is difficult because the portion of the basalt application that replaces the baseline is subjective. To get around this issue, the Isometric (2025) protocol for enhanced weathering ignores $E_{baseline}$ entirely. We adopt this method for our net CDR quantification because it is the only existing protocol we identified that clearly addresses the issue of baseline rock amendments (Kukla et al., 2024). These modifications give us the net CDR equation

$$\text{net CDR} = (R_{project} - \text{MAX}(R_{baseline}, 0)) - E_{project}. \quad (9)$$

If there is no baseline activity — *i.e.,* no liming — then $R_{baseline} = 0$ and equation 9 simplifies to net CDR $= R_{project} - E_{project}$.

3 Results and Discussion

3.1 Initial removal with basalt and calcite

Our results show that basalt carbon removal outcomes are more sensitive to both the diameter and amount of dust than calcite. Figure 1 shows the initial removal, integrated across 15 years, using equation 6 with F_{loss} set to zero. The first key distinction between basalt and calcite is that while R_{basalt} tends to increase with finer feedstock grain sizes, $R_{calcite}$ is largely insensitive to the dust diameter. Instead, calcite weathers fast enough that total dissolution depends primarily on the amount of rock available and the degree of calcite saturation in the soil. Its dissolution is not strongly limited by the available reactive surface area for a given volume of rock. This result holds for all of the surface area parameterizations we tested with calcite (Fig. S5 in Supporting Information).

In contrast to $R_{calcite}$, the magnitude of R_{basalt} is highly sensitive to how the mineral surface area is calculated and how it evolves over time (Fig. S5 in Supporting Information). For example, R_{basalt} decreases if particle size tracking is turned off and surface area is allowed to increase with porosity. If we assume the end-member case where the particles are spherical with no surface roughness, then R_{basalt} decreases further. While these same treatments have a negligible effect on $R_{calcite}$, we note that some research has found that soil pH outcomes can be sensitive to calcite particle sizes within our simulated range (Beacher & Merkle, 1949; Jones & Mallarino, 2018).

Basalt and calcite also differ in the range of initial removal outcomes. Calcite dissolution is limited by calcite saturation and, at a certain point, adding more rock leads to a negligible increase in $R_{calcite}$. The point where calcite saturation occurs, however, is sensitive to the soil water infiltration rate (Fig. S6 in Supporting Information), consistent with previous work showing a strong dependence of calcite saturation on the water-rock ratio and water balance (*e.g.,* Clow & Mast, 2010; Slessarev et al., 2016). In contrast, we do not see strong saturation impacts on R_{basalt} in our simulation conditions — R_{basalt} increases continuously with more and finer rock within the range we tested (see Fig. S7 in Supporting Information). We also note that increasing fertilizer input generally decreases R for both basalt and calcite. This result is consistent with a shift to more non-carbonic acid weathering at the expense of that driven by carbonic acid. At lower application rates in the more acidic case, calcite dissolution is dominated by non-carbonic acid. This drives $R_{calcite}$ negative, indicating that calcite-derived carbon is being released to the atmosphere. Though note that this analysis only accounts for the CO_2 budget of the soil column and ignores the fact that neutralizing non-carbonic acid is likely to decrease CO_2 evasion downstream.

When we account for a specific baseline liming practice, more or finer basalt is needed to break even with the baseline calcite removal flux in the less acidic case. Figure 2A shows

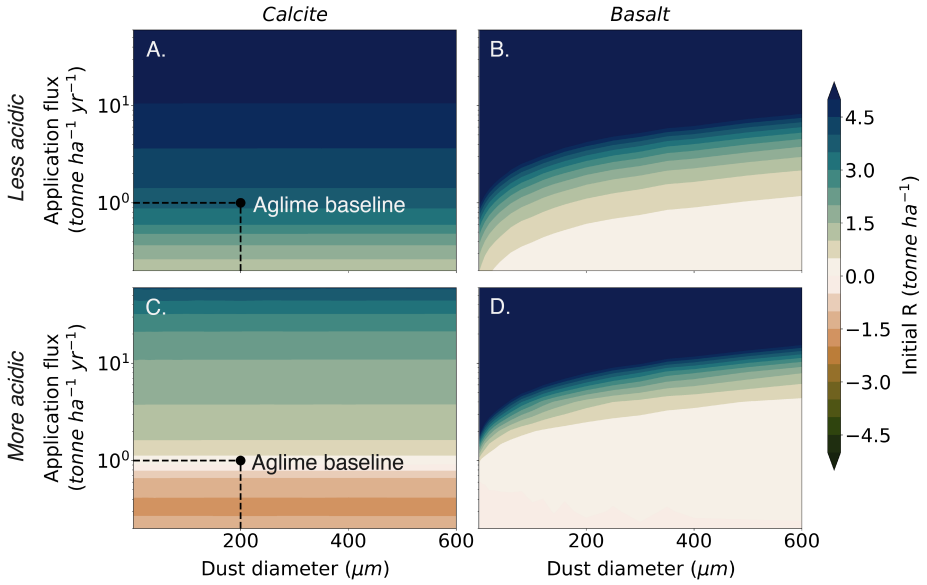

Figure 1. R_{basalt} and R_{calcite} for the less acidic case (**A**, **B**) and more acidic case (**C**, **D**). Cool colors indicate removal and warm colors indicate the net release of fossil carbon. Calcite is net-emitting in the more acidic case for low application fluxes. The baseline liming practice is the same for the less and more acidic cases and is shown by a black point in panels **A** and **C**.

the net removal flux of the basalt application compared to the baseline calcite amendment calculated using equation 7. For the same dust diameter (200 μm), the break-even line requires more than a 3x increase in rock application. This number approaches 20x if the particle size tracking is turned off (not shown), emphasizing the importance of the surface area parameterization. When the basalt is ground down to just a few microns in diameter, the break-even dips slightly below the baseline liming flux, or reaches $\sim$ 2x the baseline flux with no particle size tracking. Of course, the break-even line is sensitive to the baseline scenario (Fig. S8 in Supporting Information), but in this case the line is at the upper end of common liming practices in the Great Plains. In the more acidic case, by contrast, the break-even line is shifted lower and net R is negligible in most of the box denoting common liming practices in the Great Plains (Fig. 2B).

Importantly, because we spread rock each year throughout the 15-year time horizon, the last rock to be spread has little time to weather. This could hurt slower-weathering feedstocks, like basalt, if substantial weathering occurs after the chosen time horizon. To give basalt more time to weather, we repeat our simulations but only apply rock in the first year, letting it weather for the following 14 (Fig. S9 in Supporting Information). We find that basalt performs relatively better at low application fluxes, as both feedstocks weather nearly completely. But, compared to the yearly application case, calcite generally performs better at mid-to-high application fluxes. In this range, a smaller fraction of basalt weathers while calcite continues to weather nearly completely. When considering the trade-off between basalt and calcite, these results suggest basalt benefits more from our decision to spread rock each year throughout the time horizon.

3.2 Downstream losses and upstream emissions

On its way to a durable storage reservoir, weathering-derived DIC and alkalinity can be lost due to processes such as secondary mineral formation, carbonate system re-equilibration, river evasion, and plant cation uptake (Kanzaki et al., 2023; Neumann et

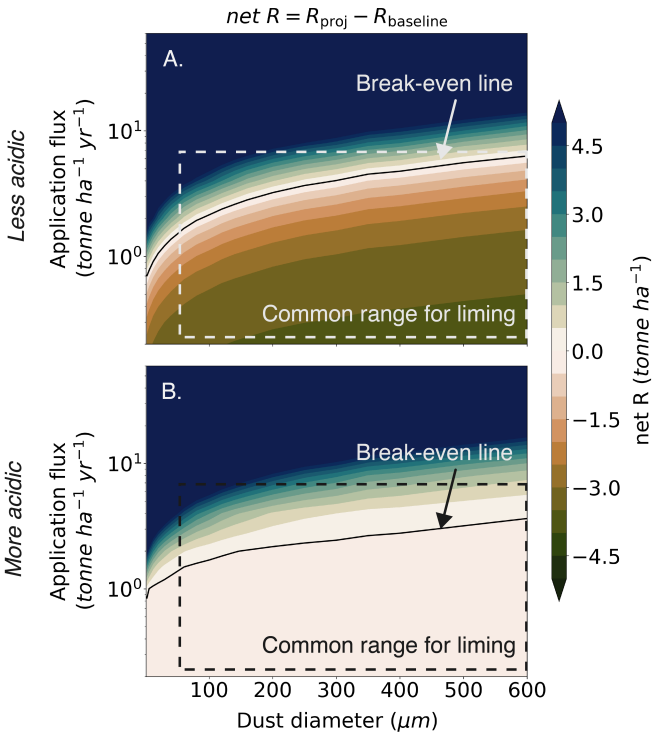

Figure 2. Basalt net removal after subtracting the effect of counterfactual liming for the less acidic case (**A**) and more acidic case (**B**). Note that R_{net} approaches R_{basalt} in panel **B** because R_{calcite} is near zero.

al., 2025; Renforth & Henderson, 2017; S. Zhang et al., 2022). Beyond the ∼10-30 cm depth where some of these processes are measured in the field, the magnitude of potential losses is poorly known. For simplicity, we prescribe the percentage of carbon lost and assume it is the same for basalt and calcite amendments (see equations 5 and 6). In reality, the losses can differ by feedstock as they release different cations and different amounts of alkalinity.

When downstream losses apply to both an enhanced weathering project and the counterfactual (or baseline), they could either decrease or increase net carbon removal (*i.e.,* net R in equation 7). Of course, when there is no counterfactual to compare to, more downstream loss decreases net R. However, when the losses affect the counterfactual more than the project, downstream loss increases net R. Importantly, that condition necessarily holds for all points on the break-even (dashed line in Fig. 3) (see Text S3 and Fig. S10 in Supporting Information). As a result, any increase in downstream loss, applied equally to the project and counterfactual, shifts the break-even line lower. In other words, a higher loss percent means carbon removal from basalt weathering balances calcite with relatively less or coarser rock. These shifts are small at first, but grow rapidly as the loss approaches the point where calcite is no longer net-removing (∼ 48% in Fig. 3A). Calcite is nearly net-emitting in the more acidic case, so $R_{\text{basalt}} > R_{\text{calcite}}$ under all conditions when the loss factor is greater than or equal to 10%. Moving forward, we apply a 10% downstream loss to basalt and calcite for all simulations unless otherwise stated.

Upstream emissions (E), by contrast, tend to shift the break-even line up and to the left in the less acidic case. Figure 3C and 3D show net $R-E$ calculated with equation 8. In the simplified, albeit improbable, case where both feedstocks are transported to the field site along the same route, sourcing the basalt is more emissions intensive be-

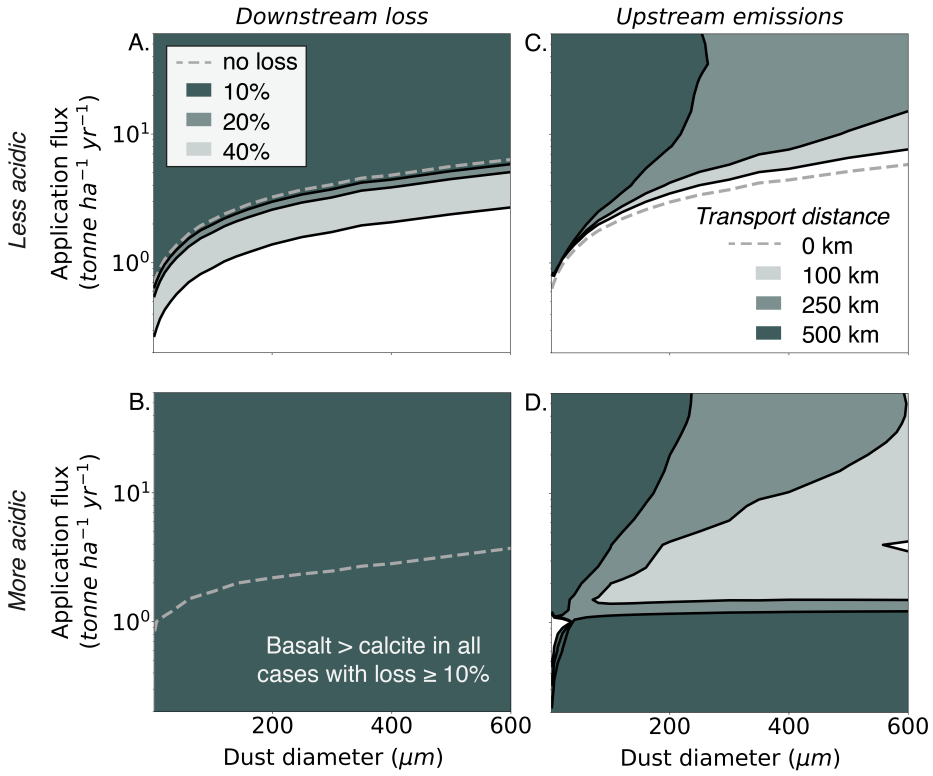

Figure 3. The effect of downstream loss percent (**A**, **B**) and upstream transport emissions (**C**, **D**) in the less acidic and more acidic cases, respectively. The lines in each panel are break-even lines where $R_{\text{basalt}} = R_{\text{calcite}}$, with $R_{\text{basalt}} > R_{\text{calcite}}$ above the line and vice versa. The shaded areas refer to regions of the solution space where the basalt amendment produces more carbon removal than the baseline calcite amendment. Basalt and calcite amendments are compared using equation 7 for panels A and B, and equation 8 for panels A and C.

cause a greater amount of rock is required and basalt's Bond work index is higher. Despite the emissions penalty, removals tend to increase faster than emissions when more basalt is added, but not when more calcite is added (Fig. S11 and S12 in Supporting Information). Notably, basalt removals do not necessarily outpace emissions when adding more rock. If particle size tracking is turned off, or the surface roughness is low, then adding more rock can increase the emissions burden faster than the removal flux (Fig. S13 in Supporting Information).

Figure 3D indicates that, as the transport distance increases, intermediate application fluxes and coarser basalt become less favorable compared to the baseline liming practice. This creates a left-facing wedge where net $R-E$ is negative. To reach a condition where net $R-E$ is positive, one could either add more and finer rock (moving up and to the left, as in Fig. 3C) or decrease the application flux to less than ~ 1 tonne ha^{-1} yr^{-1} (moving down in Fig. 3D). These two solution spaces emerge because, when we account for upstream emissions, the baseline liming practice is net emitting in the more acidic case. This drives net $R-E$ positive at low application fluxes primarily because of the decrease in E_{basalt}. In our simulations, the incomplete weathering of basalt limits R such that transport distances over ~ 750 km are generally net emitting over the 15-year time horizon, or distances over ~ 30km when particle size tracking is turned off.

3.3 Carbon accounting

Carbon accounting decisions can exert substantial influence over the perceived climate outcomes of a project. Today, essentially all enhanced rock weathering projects are financed by, or preparing to be financed by, the sale of carbon removal credits in conventional carbon markets. These removal credits must represent carbon removed from the atmosphere, excluding emissions that were avoided. This distinction recognizes the fact that removals and avoided emissions serve different purposes in reaching net-zero. Avoiding emissions helps slow climate change and represents the vast majority of the work we need to do to reach net-zero. Removals are meant to balance residual emissions and potentially remove legacy emissions.

Separating avoided emissions from removals requires carefully crafted carbon accounting rules (Nordahl et al., 2024). For example, if $E_{\text{basalt}} < E_{\text{calcite}}$, equation 8 counts the decrease in E as CDR. Equation 9, in contrast, guarantees that avoided emissions are not counted as CDR. Though equation 9 is also one-sided, accounting for baseline removals while ignoring any potential relief from baseline emissions. See Kukla et al. (2024) for more discussion on methods for separating avoided emissions and removals.

Figure 4 shows how the application conditions where basalt-driven removal exceeds calcite can depend on accounting choices. For the less acidic cases, there is not much difference between the three accounting approaches — for reference, the break-even line on panel A is copied onto panel C, and panel C on to E. The break-even line shifts upward slightly when we account for emissions (Fig. 4C), as the E_{project} required to break-even exceeds E_{baseline}. Then separating avoided emissions nudges the break-even line up a distance that is determined, in this case, by the magnitude of E_{baseline} (Fig. 4E). Since E_{baseline} is small relative E_{project}, panels C and E are nearly identical. More broadly, the similarity of panels A, C, and E is owed to the fact that R_{basalt} increases rapidly with the rock application flux, effectively bounding how much the break-even line can move. R_{basalt} increases more slowly with other surface area treatments (*e.g.,* Fig. S5 in Supporting Information), which would change the relative differences between panels A, C, and E.

In the more acidic case, R_{project} exceeds R_{baseline} everywhere (Fig. 4B) and net $R-E$ is positive almost everywhere (Fig. 4D). The two slivers of white space in Figure 4D are primarily driven by E_{project} being too high due to crushing emissions (the sliver on the left) or R_{project} being too low when an intermediate amount of coarse rock is applied. Panel F is effectively equivalent to $R_{\text{project}} - E_{\text{project}}$ because R_{baseline} is negligible.

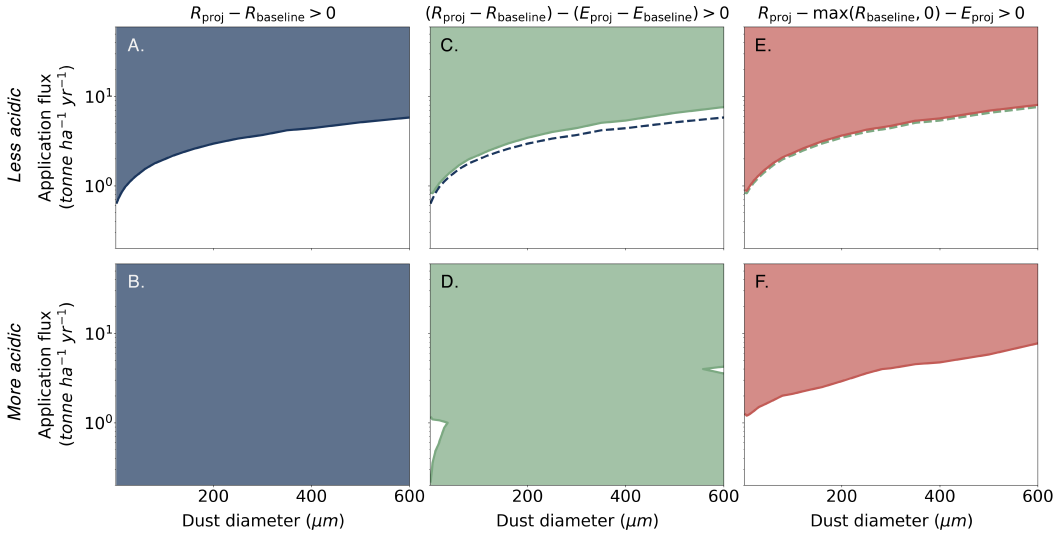

Figure 4. Shaded regions show where relative basalt carbon removal is positive for different accounting choices, including net R (**A**, **B**), net $R - E$ (**C**, **D**), and net CDR (**E**, **F**) for the less acidic and more acidic cases, respectively.

3.4 Optimizing calcite versus basalt for CDR

Given calcite's effectiveness at carbon removal, particularly in less acidic conditions, it may be more efficient to optimize calcite applications for CDR than to use basalt, even in fields with no liming history. Figure 5 compares the net CDR outcomes for basalt versus calcite amendments, accounting for upstream emissions (see Sect. 2.2) and a 10% downstream loss. In this case, there is no baseline carbon removal from counterfactual liming.

Figure 5 highlights how different decisions are required to optimize a calcite amendment for CDR compared to a basalt amendment. Calcite net CDR is highest at low-to-intermediate removal fluxes and coarser particle sizes. Adding too much calcite, or crushing it too finely, increases emissions faster than it increases removals. In contrast, more and finer basalt increases net CDR monotonically. The net CDR values change in the more acidic case, but the general shape of the solution space is similar.

Further simulations with different surface area parameterizations suggest these calcite results are more broadly generalizable, but the basalt results may not be. The shape of the calcite solution space is not sensitive to changes in the surface area parameterization (Fig. S5 in Supporting Information), which can vary from model-to-model. We expect the basic result that calcite CDR is optimized at some intermediate, relatively coarse feedstock application to hold under many conditions. The basalt results, in contrast, are highly sensitive to the surface area parameterization, with more rock driving more removal in some cases and more emissions in others (Fig. S13 in Supporting Information). The shape of this solution space likely depends on factors including the mineralogy of the feedstock, the roughness factor, the specific surface area response to weathering, and more. We cannot be confident that more and finer basalt will always drive more carbon removal.

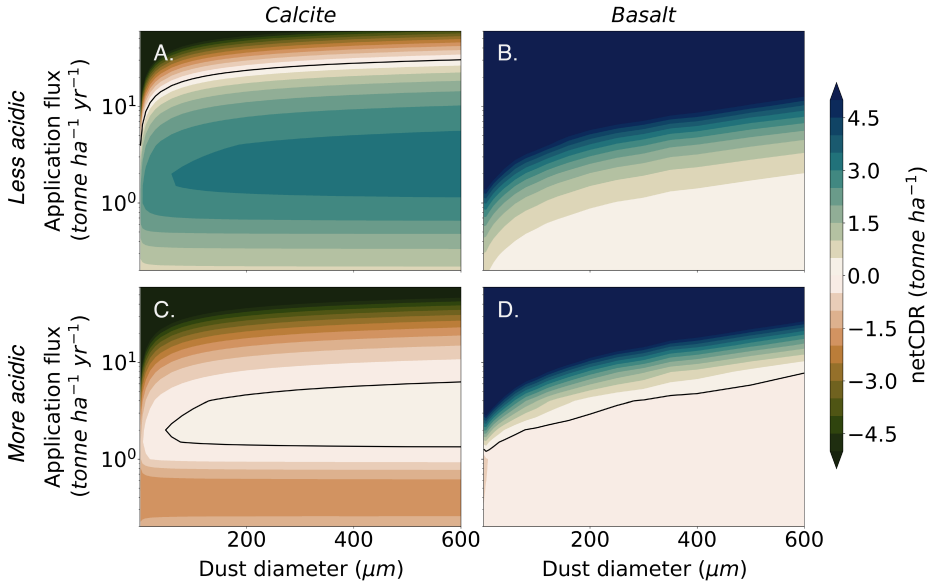

Figure 5. Net CDR for basalt and calcite when considering upstream emissions, downstream losses, and counterfactual calcite in the less acidic (**A**, **B**) and more acidic (**C**, **D**) cases. Greens indicate net removals, reds indicate net emissions. In the more acidic case, net CDR solely reflects the balance of feedstock removal and embodied emissions because the counterfactual calcite weathering emits fossil carbon.

4 Concluding remarks

Our results illustrate clear trade-offs between silicate and carbonate feedstocks for carbon removal. Carbonates weather quickly and congruently, but carry embedded fossil carbon and can saturate quickly in more water-limited environments, which could cap potential removal. Silicates weather more slowly and often incongruently, but avoid fossil carbon emissions and offer greater removal potential per unit of alkalinity. Our simulations provide additional evidence that carbonates can outperform silicates in some scenarios — particularly at lower application rates that are consistent with current agronomic practices.

Our results have a number of implications for aligning agricultural rock applications with climate goals. First, feedstock trade-offs must be carefully considered when deciding what practices to incentivize — whether selecting a rock for an enhanced weathering deployment in a context with no liming history, replacing an existing liming practice, or layering an enhanced weathering practice on top of an existing liming practice. These trade-offs are sensitive to local conditions, including pH, climate, liming history, and proximity to rock sources. While high silicate application rates can deliver strong removal outcomes, they may not be financially viable or agronomically sustainable over time (Levy et al., 2024). Carbonates, by contrast, may support more sustainable, lower-rate applications that are less likely to degrade soil properties with repeated, long-term application.

Second, any carbon removal claims must account for existing liming practices, especially in the context of carbon markets. If a new deployment is replacing or supplementing agricultural lime, then the baseline removal associated with that practice must be quantified. This is not straightforward. Baseline lime application data is not standardized and may be hard to verify, tracer-based quantification methods do not work

for most carbonates (Reershemius et al., 2023), and mechanistic models will need to confront uncertainties associated with validation, calibration, and initialization. Moreover, crediting frameworks that aim to distinguish removal from avoided emissions will have to grapple with how to handle emission reductions associated with upstream emissions or carbonate weathering that acts as a carbon source.

Third, identifying conservative accounting choices — erring on the side of less carbon removal — is more complicated when the project is weighed against a baseline scenario. For example, since downstream losses are hard to measure, common practice is to assume some loss factor or model it. Both approaches require decisions that affect carbon removal. If they are applied symmetrically to the project and the baseline, then decisions that increase loss estimates could be conservative in one project, but could inflate CDR in another. For quantification systems where conservative accounting is important, the existence of a baseline scenario requires a more careful consideration of each accounting choice.

This work presents a framework for evaluating carbon removal trade-offs between silicate and carbonate feedstocks, taking into account site-specific conditions, rock quantity and particle size, upstream emissions, and downstream losses. While we focus on mechanistic modeling of carbon removal at the field scale, future work should incorporate other greenhouse gases, more detailed representations of downstream geochemistry, and comparatively evaluate the framework with other reaction-transport codes. This analysis is a first step toward supporting more nuanced feedstock choices — both in the context of carbon market projects and with respect to broader policy efforts aimed at incentivizing the use of rock dust in agricultural soil pH management.

5 Open Research

Datasets associated with this manuscript are available under a CC-BY 4.0 license (Kukla, 2025). Code for reproducing the analysis, setting up SCEPTER simulations, and processing the output is available under MIT license here: `https://github.com/carbonplan/ew-workflows/releases/tag/v1.0`. Code for SCEPTER is available under a GPL 3.0 license here: `https://github.com/cdr-laboratory/SCEPTER/releases/tag/v1.0.1`.

Acknowledgments

TK thanks Brian Rogers for helpful conversations that improved the text. TK was supported in part by grants to CarbonPlan from Giving Green (via Giving What We Can) and Adam and Abigail Winkel. CTR and NJP were supported in part by the Grantham Foundation for the Environment and the US Department of Energy. NJP was a co-founder of Lithos Carbon and CREW Carbon but has no financial ties to these companies. CTR was a co-founder of Lithos Carbon, but has no financial ties to the company. CTR serves as a scientific advisor to CREW Carbon. TK and YK declare no competing interests.

References

Baek, S. H., Kanzaki, Y., Lora, J. M., Planavsky, N., Reinhard, C. T., & Zhang, S. (2023, August). Impact of Climate on the Global Capacity for Enhanced Rock Weathering on Croplands. *Earth's Future*, *11*(8), e2023EF003698. doi: 10.1029/2023EF003698

Beacher, R. L., & Merkle, F. G. (1949, January). The Influence of Form and Fineness of Lime Compounds Upon the Correction of Acidity and Upon the Nutrient Status of Soils. *Soil Science Society of America Journal*, *13*(C), 391–393. doi: 10.2136/sssaj1949.036159950013000C0071x

Beerling, D. J., Epihov, D. Z., Kantola, I. B., Masters, M. D., Reershemius, T., Planavsky, N. J., ... Banwart, S. A. (2024, February). Enhanced weath-

ering in the US Corn Belt delivers carbon removal with agronomic benefits. *Proceedings of the National Academy of Sciences*, *121*(9), e2319436121. doi: 10.1073/pnas.2319436121

Beerling, D. J., Kantzas, E. P., Lomas, M. R., Taylor, L. L., Zhang, S., Kanzaki, Y., ... Val Martin, M. (2025, February). Transforming US agriculture for carbon removal with enhanced weathering. *Nature*. doi: 10.1038/s41586-024-08429-2

Beerling, D. J., Leake, J. R., Long, S. P., Scholes, J. D., Ton, J., Nelson, P. N., ... Hansen, J. (2018, February). Farming with crops and rocks to address global climate, food and soil security. *Nature Plants*, *4*(3), 138–147. doi: 10.1038/s41477-018-0108-y

Bond, F. C. (1961). Crushing and grinding calculations, part I. *British Chemical Engineering*, *6*, 378–385.

Buckingham, F., & Henderson, G. (2024, January). The enhanced weathering potential of a range of silicate and carbonate additions in a UK agricultural soil. *Science of The Total Environment*, *907*, 167701. doi: 10.1016/j.scitotenv.2023.167701

Campolongo, F., Cariboni, J., & Saltelli, A. (2007, October). An effective screening design for sensitivity analysis of large models. *Environmental Modelling & Software*, *22*(10), 1509–1518. doi: 10.1016/j.envsoft.2006.10.004

Cao, P., Lu, C., & Yu, Z. (2018, June). Historical nitrogen fertilizer use in agricultural ecosystems of the contiguous United States during 1850–2015: Application rate, timing, and fertilizer types. *Earth System Science Data*, *10*(2), 969–984. doi: 10.5194/essd-10-969-2018

Clow, D. W., & Mast, M. A. (2010, January). Mechanisms for chemostatic behavior in catchments: Implications for CO2 consumption by mineral weathering. *Chemical Geology*, *269*(1-2), 40–51. doi: 10.1016/j.chemgeo.2009.09.014

Dietzen, C., Harrison, R., & Michelsen-Correa, S. (2018, July). Effectiveness of enhanced mineral weathering as a carbon sequestration tool and alternative to agricultural lime: An incubation experiment. *International Journal of Greenhouse Gas Control*, *74*, 251–258. doi: 10.1016/j.ijggc.2018.05.007

Dreybrodt, W. (1988). *Processes in Karst Systems* (Vol. 4; D. Barsch, I. Douglas, F. Joly, M. Marcus, & B. Messerli, Eds.). Berlin, Heidelberg: Springer Berlin Heidelberg. doi: 10.1007/978-3-642-83352-6

Dreybrodt, W., Lauckner, J., Liu, Z., Svensson, U., & Buhmann, D. (1996). The kinetics of the reaction CO2 + Hz0 + H + + HCO, as one of the rate limiting steps for the dissolution of calcite in the system H,O-COz-CaC03. *Geochimica et Cosmochimica Acta*, *60*(18), 3375–3381.

Fornara, D. A., Steinbeiss, S., McNAMARA, N. P., Gleixner, G., Oakley, S., Poulton, P. R., ... Bardgett, R. D. (2011, May). Increases in soil organic carbon sequestration can reduce the global warming potential of long-term liming to permanent grassland: Liming effects on soil carbon sequestration. *Global Change Biology*, *17*(5), 1925–1934. doi: 10.1111/j.1365-2486.2010.02328.x

Fuhr, M., Dale, A. W., Wallmann, K., Bährle, R., Kalapurakkal, H. T., Sommer, S., ... Geilert, S. (2025, February). Calcite is an efficient and low-cost material to enhance benthic weathering in shelf sediments of the Baltic Sea. *Communications Earth & Environment*, *6*(1), 106. doi: 10.1038/s43247-025-02079-6

Gaillardet, J., Calmels, D., Romero-Mujalli, G., Zakharova, E., & Hartmann, J. (2019, November). Global climate control on carbonate weathering intensity. *Chemical Geology*, *527*, 118762. doi: 10.1016/j.chemgeo.2018.05.009

Gaillardet, J., Dupré, B., Louvat, P., & Allègre, C. (1999, July). Global silicate weathering and CO2 consumption rates deduced from the chemistry of large rivers. *Chemical Geology*, *159*(1-4), 3–30. doi: 10.1016/S0009-2541(99)00031-5

Godsey, C. B., Pierzynski, G. M., Mengel, D. B., & Lamond, R. E. (2007, May). Management of Soil Acidity in No-Till Production Systems through

Surface Application of Lime. *Agronomy Journal*, *99*(3), 764–772. doi: 10.2134/agronj2006.0078

Grover, S. P., Butterly, C. R., Wang, X., & Tang, C. (2017, May). The short-term effects of liming on organic carbon mineralisation in two acidic soils as affected by different rates and application depths of lime. *Biology and Fertility of Soils*, *53*(4), 431–443. doi: 10.1007/s00374-017-1196-y

Hamilton, S. K., Kurzman, A. L., Arango, C., Jin, L., & Robertson, G. P. (2007, June). Evidence for carbon sequestration by agricultural liming: Fate of carbon in agricultural lime. *Global Biogeochemical Cycles*, *21*(2), n/a-n/a. doi: 10.1029/2006GB002738

Haque, F., Santos, R. M., & Chiang, Y. W. (2020, July). Optimizing Inorganic Carbon Sequestration and Crop Yield With Wollastonite Soil Amendment in a Microplot Study. *Frontiers in Plant Science*, *11*, 1012. doi: 10.3389/fpls.2020.01012

Hartmann, J., West, A. J., Renforth, P., Köhler, P., De La Rocha, C. L., Wolf-Gladrow, D. A., ... Scheffran, J. (2013, April). Enhanced chemical weathering as a geoengineering strategy to reduce atmospheric carbon dioxide, supply nutrients, and mitigate ocean acidification: ENHANCED WEATHERING. *Reviews of Geophysics*, *51*(2), 113–149. doi: 10.1002/rog.20004

Herman, J., & Usher, W. (2017, January). SALib: An open-source Python library for Sensitivity Analysis. *The Journal of Open Source Software*, *2*(9), 97. doi: 10.21105/joss.00097

Isometric. (2025). *Enhanced weathering in agriculture v1.1.* Author.

Iwanaga, T., Usher, W., & Herman, J. (2022, May). Toward SALib 2.0: Advancing the accessibility and interpretability of global sensitivity analyses. *Socio-Environmental Systems Modelling*, *4*, 18155. doi: 10.18174/sesmo.18155

Jones, J. D., & Mallarino, A. P. (2018, January). Influence of Source and Particle Size on Agricultural Limestone Efficiency at Increasing Soil pH. *Soil Science Society of America Journal*, *82*(1), 271–282. doi: 10.2136/sssaj2017.06.0207

Kanda, Y., & Kotake, N. (2007). Chapter 12 Comminution Energy and Evaluation in Fine Grinding. In *Handbook of Powder Technology* (Vol. 12, pp. 529–550). Elsevier. doi: 10.1016/S0167-3785(07)12015-7

Kantola, I. B., Blanc-Betes, E., Masters, M. D., Chang, E., Marklein, A., Moore, C. E., ... DeLucia, E. H. (2023, August). Improved net carbon budgets in the US Midwest through direct measured impacts of enhanced weathering. *Global Change Biology*, gcb.16903. doi: 10.1111/gcb.16903

Kanzaki, Y., Chiaravalloti, I., Zhang, S., Planavsky, N. J., & Reinhard, C. T. (2024, May). In silico calculation of soil pH by SCEPTER v1.0. *Geoscientific Model Development*, *17*(10), 4515–4532. doi: 10.5194/gmd-17-4515-2024

Kanzaki, Y., Planavsky, N. J., & Reinhard, C. T. (2023, April). New estimates of the storage permanence and ocean co-benefits of enhanced rock weathering. *PNAS Nexus*, *2*(4), pgad059. doi: 10.1093/pnasnexus/pgad059

Kanzaki, Y., Planavsky, N. J., Zhang, S., Jordan, J., Suhrhoff, T. J., & Reinhard, C. T. (2025, July). Soil cation storage is a key control on the carbon removal dynamics of enhanced weathering. *Environmental Research Letters*, *20*(7), 074055. doi: 10.1088/1748-9326/ade0d5

Kanzaki, Y., Zhang, S., Planavsky, N. J., & Reinhard, C. T. (2022, June). Soil Cycles of Elements simulator for Predicting TERrestrial regulation of greenhouse gases: SCEPTER v0.9. *Geoscientific Model Development*, *15*(12), 4959–4990. doi: 10.5194/gmd-15-4959-2022

Kukla, T. (2025). *Data for: Swapping carbonate for silicate in agricultural enhanced rock weathering (1.0).* Zenodo. doi: 10.5281/zenodo.16916118

Kukla, T., Loeffler, S., Martin, K., & Chay, F. (2024). *Crediting challenges when carbon removal comes with avoided emissions.* CarbonPlan.

Lentz, E. M., Diedrick, K. A., Dygert, C. E., Henry, D. C., & Mullen, R. W. (2010).

Soil pH and corn grain yield response to low rates of pelletized lime and typical aglime. *Journal of the National Association of County Agricultural Agents*, *3*(1).

Lerman, A., & Wu, L. (2006, January). CO2 and sulfuric acid controls of weathering and river water composition. *Journal of Geochemical Exploration*, *88*(1-3), 427–430. doi: 10.1016/j.gexplo.2005.08.100

Levy, C. R., Almaraz, M., Beerling, D. J., Raymond, P., Reinhard, C. T., Suhrhoff, T. J., & Taylor, L. (2024, September). Enhanced Rock Weathering for Carbon Removal–Monitoring and Mitigating Potential Environmental Impacts on Agricultural Land. *Environmental Science & Technology*, acs.est.4c02368. doi: 10.1021/acs.est.4c02368

Li, Z., Planavsky, N. J., & Reinhard, C. T. (2024, August). Geospatial assessment of the cost and energy demand of feedstock grinding for enhanced rock weathering in the coterminous United States. *Frontiers in Climate*, *6*, 1380651. doi: 10.3389/fclim.2024.1380651

Lu, C., & Tian, H. (2017). Global nitrogen and phosphorus fertilizer use for agriculture production in the past half century: Shifted hot spots and nutrient imbalance.

Mallarino, A. P., Sawyer, J. E., Barnhart, S. K., & Licht, M. A. (2023). *A General Guide for Crop Nutrient and Limestone Recommendations in Iowa.* Iowa State University Extension and Outreach.

Moon, S., Chamberlain, C., & Hilley, G. (2014, June). New estimates of silicate weathering rates and their uncertainties in global rivers. *Geochimica et Cosmochimica Acta*, *134*, 257–274. doi: 10.1016/j.gca.2014.02.033

Morris, M. D. (1991). Factorial Sampling Plans for Preliminary Computational Experiments. *Technometrics*, *33*(2). doi: 10.1080/00401706.1991.10484804

Navarre-Sitchler, A., & Brantley, S. (2007, September). Basalt weathering across scales. *Earth and Planetary Science Letters*, *261*(1-2), 321–334. doi: 10.1016/j.epsl.2007.07.010

Neumann, R. B., Kukla, T., Zhang, S., & Butman, D. E. (2025). Riverine photosynthesis influences the carbon sequestration potential of enhanced rock weathering. *Frontiers in Climate*, *7*. doi: 10.3389/fclim.2025.1582786

Nishina, K., Ito, A., Hanasaki, N., & Hayashi, S. (2017). Reconstruction of spatially detailed global map of NH+4 and NO-3 application in synthetic nitrogen fertilizer.

Nordahl, S. L., Hanes, R. J., Mayfield, K. K., Myers, C., Baker, S. E., & Scown, C. D. (2024, September). Carbon accounting for carbon dioxide removal. *One Earth*, *7*(9), 1494–1500. doi: 10.1016/j.oneear.2024.08.012

Oh, N.-H., & Raymond, P. A. (2006, September). Contribution of agricultural liming to riverine bicarbonate export and CO $_2$ sequestration in the Ohio River basin: Liming effects on riverine bicarbonate export. *Global Biogeochemical Cycles*, *20*(3), n/a-n/a. doi: 10.1029/2005GB002565

Pagani, A., & Mallarino, A. P. (2012, September). Soil pH and Crop Grain Yield as Affected by the Source and Rate of Lime. *Soil Science Society of America Journal*, *76*(5), 1877–1886. doi: 10.2136/sssaj2012.0119

Perrin, A.-S., Probst, A., & Probst, J.-L. (2008, July). Impact of nitrogenous fertilizers on carbonate dissolution in small agricultural catchments: Implications for weathering CO2 uptake at regional and global scales. *Geochimica et Cosmochimica Acta*, *72*(13), 3105–3123. doi: 10.1016/j.gca.2008.04.011

Raymond, P. A., Planavsky, N. J., & Reinhard, C. T. (in press). Using carbonates for carbon removal. *Nature Water*.

Reershemius, T., Kelland, M. E., Jordan, J. S., Davis, I. R., D'Ascanio, R., Kalderon-Asael, B., ... Planavsky, N. J. (2023, November). Initial Validation of a Soil-Based Mass-Balance Approach for Empirical Monitoring of Enhanced Rock Weathering Rates. *Environmental Science & Technology*, acs.est.3c03609.

doi: 10.1021/acs.est.3c03609

Renforth, P., & Henderson, G. (2017, September). Assessing ocean alkalinity for carbon sequestration: Ocean Alkalinity for C Sequestration. *Reviews of Geophysics*, *55*(3), 636–674. doi: 10.1002/2016RG000533

Ruano, M., Ribes, J., Seco, A., & Ferrer, J. (2012, November). An improved sampling strategy based on trajectory design for application of the Morris method to systems with many input factors. *Environmental Modelling & Software*, *37*, 103–109. doi: 10.1016/j.envsoft.2012.03.008

Schuiling, R. D., Wilson, S., & Power, L. M. (2011, March). Enhanced silicate weathering is not limited by silicic acid saturation. *Proceedings of the National Academy of Sciences*, *108*(12). doi: 10.1073/pnas.1019024108

Slessarev, E. W., Lin, Y., Bingham, N. L., Johnson, J. E., Dai, Y., Schimel, J. P., & Chadwick, O. A. (2016, December). Water balance creates a threshold in soil pH at the global scale. *Nature*, *540*(7634), 567–569. doi: 10.1038/nature20139

Suarez, D. L., & Rhoades, J. D. (1982, July). The Apparent Solubility of Calcium Carbonate in Soils. *Soil Science Society of America Journal*, *46*(4), 716–722. doi: 10.2136/sssaj1982.03615995004600040010x

Vienne, A., Poblador, S., Portillo-Estrada, M., Hartmann, J., Ijiehon, S., Wade, P., & Vicca, S. (2022, May). Enhanced Weathering Using Basalt Rock Powder: Carbon Sequestration, Co-benefits and Risks in a Mesocosm Study With Solanum tuberosum. *Frontiers in Climate*, *4*, 869456. doi: 10.3389/fclim.2022.869456

Wang, Y., Yao, Z., Zhan, Y., Zheng, X., Zhou, M., Yan, G., ... Butterbach-Bahl, K. (2021, June). Potential benefits of liming to acid soils on climate change mitigation and food security. *Global Change Biology*, *27*(12), 2807–2821. doi: 10.1111/gcb.15607

West, T. O., & McBride, A. C. (2005, June). The contribution of agricultural lime to carbon dioxide emissions in the United States: Dissolution, transport, and net emissions. *Agriculture, Ecosystems & Environment*, *108*(2), 145–154. doi: 10.1016/j.agee.2005.01.002

Zamanian, K., Zhou, J., & Kuzyakov, Y. (2021, February). Soil carbonates: The unaccounted, irrecoverable carbon source. *Geoderma*, *384*, 114817. doi: 10.1016/j.geoderma.2020.114817

Zhang, B., Kroeger, J., Planavsky, N., & Yao, Y. (2023, September). Techno-Economic and Life Cycle Assessment of Enhanced Rock Weathering: A Case Study from the Midwestern United States. *Environmental Science & Technology*, *57*(37), 13828–13837. doi: 10.1021/acs.est.3c01658

Zhang, H.-M., Liang, Z., Li, Y., Chen, Z.-X., Zhang, J.-B., Cai, Z.-C., ... Abalos, D. (2022, December). Liming modifies greenhouse gas fluxes from soils: A meta-analysis of biological drivers. *Agriculture, Ecosystems & Environment*, *340*, 108182. doi: 10.1016/j.agee.2022.108182

Zhang, S., Planavsky, N. J., Katchinoff, J., Raymond, P. A., Kanzaki, Y., Reershemius, T., & Reinhard, C. T. (2022, November). River chemistry constraints on the carbon capture potential of surficial enhanced rock weathering. *Limnology and Oceanography*, *67*(S2). doi: 10.1002/lno.12244

Supporting Information for "Swapping carbonate for silicate in agricultural enhanced rock weathering"

Tyler Kukla[1], Yoshiki Kanzaki[2], Freya Chay[1], Noah J. Planavsky[3,4],

Christopher T. Reinhard[2]

[1]CarbonPlan, San Francisco, CA, USA

[2]School of Earth and Atmospheric Sciences, Georgia Institute of Technology, Atlanta, GA, USA

[3]Department of Earth and Planetary Sciences, Yale University, New Haven, CT, USA

[4]Yale Center for Natural Carbon Capture, New Haven, CT, USA

Contents of this file

Text S1: SCEPTER gas-phase mass balance

SCEPTER tracks the partial pressure (p_ε; atm) of a gas species ε based on its production or consumption by solid and aqueous phases, its diffusive transport in the gas phase and dissolved phase, and its advective transport in the dissolved phase. The governing equation for the gas-phase mass balance is

$$\frac{\partial \alpha_\varepsilon p_\varepsilon}{\partial t} = -\frac{\partial \phi \sigma \ell v H_\varepsilon p_\varepsilon}{\partial z} + \frac{\partial}{\partial z}\left(D_\varepsilon^{\text{eff}} \frac{\partial p_\varepsilon}{\partial z}\right) + \sum_\theta^{n_{\text{sld}}} \gamma_{\theta,\varepsilon} R_\theta + \sum_\kappa^{n_{\text{xrxn}}} \gamma_{\kappa,\varepsilon} R_\kappa. \quad (1)$$

Here, ε denotes a particular gas species, θ is a particular solid species, κ is a user-defined "extra" reaction, t is time (s), z is depth (m), and α_ε is a unit conversion factor (mol m^{-3} atm^{-1}) (see equation S2). The first two terms on the right hand side of equation 1 represent the advection of dissolved gas and diffusion of all gas (including dissolved), respectively, and the second two terms represent the net gas production due to reactions with solids and extra reactions, respectively.

In the advection term of equation S1, ϕ is the soil porosity, σ is the soil water saturation, ℓ converts liters to cubic meters, v is the rate of downward porewater advection (m yr^{-1}), and H_ε is the solubility of the gas species (mol L^{-1} atm^{-1}). The diffusion term relies on an effective diffusion coefficient, $D_\varepsilon^{\text{eff}}$ (mol atm^{-1} m^{-1} yr^{-1}) which accounts for diffusion in the gas phase and the aqueous dissolved gas phase (see equation S3 below). The net production of gas ε from solid species θ is $\gamma_{\theta,\varepsilon}$ (mol), and R_θ is the net dissolution rate of θ (mol m^{-3} yr^{-1}). The net production from extra reaction κ depends on the stoichiometric coefficient of ε in the reaction, $\gamma_{\theta,\varepsilon}$ and the reaction rate R_κ (mol m^{-3} yr^{-1}). We note that the reaction rates are represented as R here for consistency with Kanzaki, Zhang, Planavsky, and Reinhard (2022), but should not be confused with initial CDR R in the main text (e.g., equation 6).

In order to track the transport of gas, including its dissolved component, equation S1 uses the conversion factor α_ε and the effective (gas plus aqueous) diffusion coefficient $D_\varepsilon^{\text{eff}}$,

defined as

$$\alpha_{\varepsilon} = \eta\phi\,(1-\sigma)\,\ell + \phi\sigma\ell H_{\varepsilon} \tag{2}$$

and

$$D_{\varepsilon}^{\mathrm{eff}} = \eta\phi\,(1-\sigma)\,\ell\tau_{\mathrm{gas}} D_{\varepsilon}^{\mathrm{gas}} + \phi\sigma\ell H_{\varepsilon}\tau_{\mathrm{aq}} D_{\varepsilon}^{\mathrm{aq}}. \tag{3}$$

Here, η is a factor for converting atm to molarity, τ_{gas} is the tortuosity factor for gas diffusion in unsaturated pore space, $D_{\varepsilon}^{\mathrm{gas}}$ is the diffusion coefficient for gas phases of ε and $D_{\varepsilon}^{\mathrm{aq}}$ is the coefficient for aqueous phases ($\mathrm{m}^2\ \mathrm{yr}^{-1}$).

In our simulations, the advection and diffusion terms of equation S1 correspond to F_{adv} and F_{dif} in the soil $p\mathrm{CO}_2$ mass balance, respectively (see equation 5 of the main text). F_{org} and F_{inorg} capture all of the non-zero solid phase contributions to soil $p\mathrm{CO}_2$, such that the sum of F_{org} and F_{inorg} is equal to the solid phase net production term in equation S1. We do not include any extra reactions beyond SCEPTER's default reactions, so the extra reaction term in equation S1 goes to zero.

Text S2: SCEPTER sensitivity analysis

We test the sensitivity of model results to eight key input parameters listed in table S2. All SCEPTER simulations for our sensitivity analysis are run for 5 years with annual rock application of either basalt or calcite. We turn off particle size tracking in these simulations to improve computational efficiency. CDR is calculated relative to a no-application (of rock or fertilizer) control simulation.

We use the Morris method, as implemented in the SALib python package (v1.4.7) for our sensitivity analysis (Campolongo et al., 2007; Herman & Usher, 2017; Iwanaga et al., 2022; Morris, 1991; Ruano et al., 2012). The Morris method is a global, elementary effects method that nudges one input parameter at a time. It outputs metrics for the direction, magnitude, and standard deviation of the effects — the latter being indicator for interactions with other inputs. We chose this method because the results are straightforward to interpret and it is computationally inexpensive to run, often requiring 100s rather than 1000s of simulations or more.

We generated 450 sets of input parameters using the Morris sampler in the SALib package. To generate these inputs, we sampled four input levels across 50 optimal trajectories that were selected from a random sample of 750 trajectories using local (rather than global) optimization. Using the results from 900 simulations (450 each for basalt and calcite) we computed sensitivity metrics for the initial CDR (R_{X}) as well as the difference between R_{basalt} and R_{calcite}. We computed sensitivity metrics these outcomes integrated over 5 years of dust application.

There are two main takeaways from our sensitivity analysis relevant to this work. First, the effect of climate forcing (*e.g.,* mean annual temperature and the soil water infiltration rate) on initial CDR outcomes is comparable to that of the annual application rate and dust grain size. This result holds for calcite, basalt, and the difference between them,

indicating that local climate conditions play an important role in the trade-offs between the feedstocks. Second, other deployment conditions such as the depth and duration of rock spreading have a relatively small effect on CDR outcomes in the model.

Given the importance of climate inputs for carbon removal outcomes, we repeated our simulations across application fluxes and dust diameters for high soil water infiltration and high mean annual temperature. We raised the infiltration rate to 1.75 m yr^{-1} and the mean annual temperature to 30^{o}C (Supporting Fig. S6). The soil water infiltration rate has a large positive effect on calcite-driven removal, consistent with previous results that show a strong dependence of calcite saturation on the water-rock ratio and water balance (Clow & Mast, 2010; Slessarev et al., 2016). Water infiltration has a more complicated effect on basalt removal, increasing it in some places and decreasing it in others. In contrast, temperature has a large positive effect on basalt-driven removal and a weak, negative effect on calcite (*e.g.,* Gaillardet et al., 2019).

Text S3: Conservative accounting of downstream losses

When tweaking an existing rock amendment for carbon dioxide removal (CDR), an assumed downstream loss fraction might apply to both the project and the counterfactual (what would have happened without the project). Therefore, it is not immediately clear whether a higher or lower assumed loss fraction is conservative (erring on the side of crediting less CDR).

To build intuition for the effect of downstream loss on net CDR, assume the total carbon exported from the field, Γ, is proportional to R by

$$\Gamma_X = \frac{R_X}{\beta_X}. \tag{4}$$

Here, subscript X is a stand-in for the rock amendment (silicate "sil" or carbonate "carb") and β is a removal efficiency coefficient denoting the fraction of total carbon export that represents carbon removed from the atmosphere. For simplicity, we set β_{sil} to 1 and β_{carb} to 0.5. This assumes the silicate feedstock carries no fossil carbon and the carbonate feedstock removes carbon at the theoretical maximum rate of 1 mole of atmospheric carbon per mole of Ca^{2+} released.

We can then apply downstream loss as a fraction, α, of total export, Γ. The effect on net CDR can be calculated as:

$$\text{CDR}_{\text{net}} = R_{\text{sil}} - \alpha\Gamma_{\text{sil}} - \text{MAX}\left(R_{\text{carb}} - \alpha\Gamma_{\text{carb}}, 0\right). \tag{5}$$

We test the effect of varying α from zero to one in three different cases: $\Gamma_{\text{sil}} = \beta_{\text{carb}}\Gamma_{\text{carb}}$ (the break-even line); $\Gamma_{\text{sil}} = \Gamma_{\text{carb}}$; and $\Gamma_{\text{sil}} = 2\Gamma_{\text{carb}}$ (Fig. S10). In the range where $\alpha > \beta_{\text{carb}}$, increasing α always results in less net CDR. When $\alpha < \beta_{\text{carb}}$, the effect of α depends on whether total carbon export, Γ, is higher for the silicate or carbonate feedstock. If Γ_{sil} is higher then raising α decreases net CDR (Fig. S10, light blue line). If

Γ_{sil} is lower, then α increases net CDR (Fig. S10, dark blue line). And if $\Gamma_{sil} = \Gamma_{carb}$ then α has no effect on net CDR.

These results indicate that, at the break-even line, increasing α up to β_{carb} will increase net CDR. This holds true as long as $\beta_{carb} < \beta_{sil}$ and both are positive. As a result, the break-even line shifts to lower application rates and coarser rock as α increases (main text Fig. 3). In contrast, α will decrease net CDR further above the break-even line where $\Gamma_{sil} > \Gamma_{carb}$.

References

Campolongo, F., Cariboni, J., & Saltelli, A. (2007, October). An effective screening design for sensitivity analysis of large models. *Environmental Modelling & Software*, *22*(10), 1509–1518. doi: 10.1016/j.envsoft.2006.10.004

Clow, D. W., & Mast, M. A. (2010, January). Mechanisms for chemostatic behavior in catchments: Implications for CO2 consumption by mineral weathering. *Chemical Geology*, *269*(1-2), 40–51. doi: 10.1016/j.chemgeo.2009.09.014

Gaillardet, J., Calmels, D., Romero-Mujalli, G., Zakharova, E., & Hartmann, J. (2019, November). Global climate control on carbonate weathering intensity. *Chemical Geology*, *527*, 118762. doi: 10.1016/j.chemgeo.2018.05.009

Herman, J., & Usher, W. (2017, January). SALib: An open-source Python library for Sensitivity Analysis. *The Journal of Open Source Software*, *2*(9), 97. doi: 10.21105/joss.00097

Iwanaga, T., Usher, W., & Herman, J. (2022, May). Toward SALib 2.0: Advancing the accessibility and interpretability of global sensitivity analyses. *Socio-Environmental Systems Modelling*, *4*, 18155. doi: 10.18174/sesmo.18155

Kanzaki, Y., Zhang, S., Planavsky, N. J., & Reinhard, C. T. (2022, June). Soil Cycles of Elements simulator for Predicting TERrestrial regulation of greenhouse gases: SCEPTER v0.9. *Geoscientific Model Development*, *15*(12), 4959–4990. doi: 10.5194/gmd-15-4959-2022

Li, Z., Planavsky, N. J., & Reinhard, C. T. (2024, August). Geospatial assessment of the cost and energy demand of feedstock grinding for enhanced rock weathering in the coterminous United States. *Frontiers in Climate*, *6*, 1380651. doi: 10.3389/fclim.2024.1380651

Morris, M. D. (1991). Factorial Sampling Plans for Preliminary Computational Experi-

ments. *Technometrics*, *33*(2). doi: 10.1080/00401706.1991.10484804

Navarre-Sitchler, A., & Brantley, S. (2007, September). Basalt weathering across scales. *Earth and Planetary Science Letters*, *261*(1-2), 321–334. doi: 10.1016/j.epsl.2007.07.010

Ruano, M., Ribes, J., Seco, A., & Ferrer, J. (2012, November). An improved sampling strategy based on trajectory design for application of the Morris method to systems with many input factors. *Environmental Modelling & Software*, *37*, 103–109. doi: 10.1016/j.envsoft.2012.03.008

Slessarev, E. W., Lin, Y., Bingham, N. L., Johnson, J. E., Dai, Y., Schimel, J. P., & Chadwick, O. A. (2016, December). Water balance creates a threshold in soil pH at the global scale. *Nature*, *540*(7634), 567–569. doi: 10.1038/nature20139

Zhang, B., Kroeger, J., Planavsky, N., & Yao, Y. (2023, September). Techno-Economic and Life Cycle Assessment of Enhanced Rock Weathering: A Case Study from the Midwestern United States. *Environmental Science & Technology*, *57*(37), 13828–13837. doi: 10.1021/acs.est.3c01658

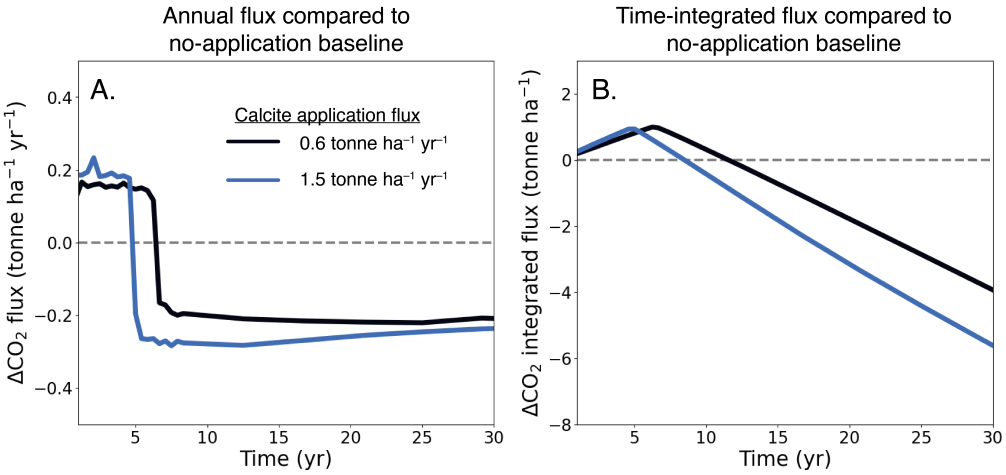

Figure S1. Time dynamics of carbon fluxes due to liming with cation exchange turned on in the model. (**A**) On an un-limed soil, calcite application is initially a carbon source and later, when the exchange sites are saturated, a carbon sink. The timing of the turnover point depends on the application flux. (**B**) The time-integrated carbon flux shows that it takes about 8 years for net carbon removal to begin in the higher application case, and about 12 years in the lower application case.

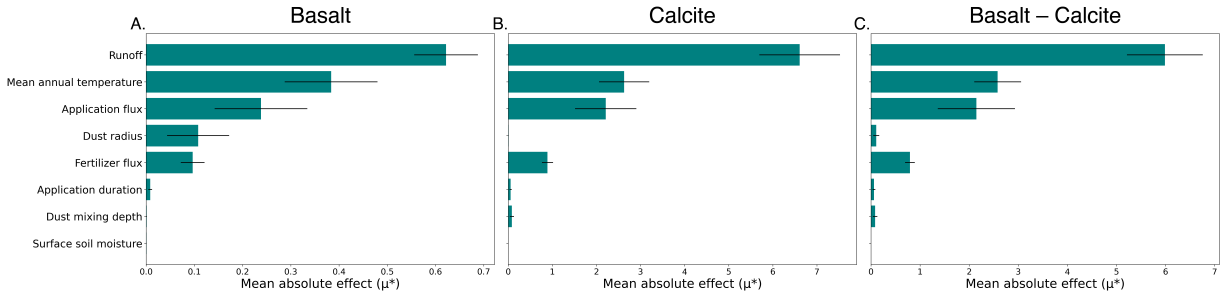

Figure S2. Morris sensitivity analysis results for the magnitude of parameter effects. In a 5-year time horizon, runoff and mean annual temperature have the largest effects on basalt (**A**), calcite (**B**), and basalt minus calcite (**C**) removal fluxes.

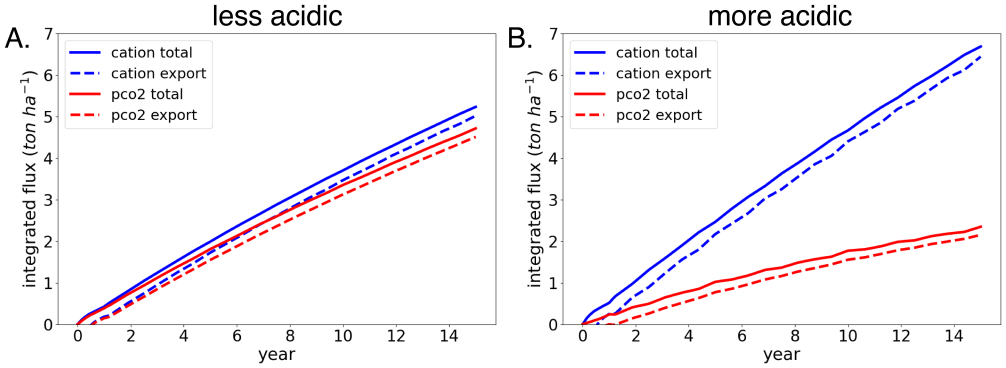

Figure S3. Calcite amendment comparison between cation-derived potential CDR (blue lines) and CO_2-derived actual CDR (red lines) for the less acidic (**A**) and more acidic (**B**) soils. As weathering mediated by strong acids makes up a larger portion of total weathering, the CO_2-derived CDR becomes a smaller portion of the potential CDR. Note, the potential CDR calculation assumes all additional cations are charge balanced by bicarbonate ions.

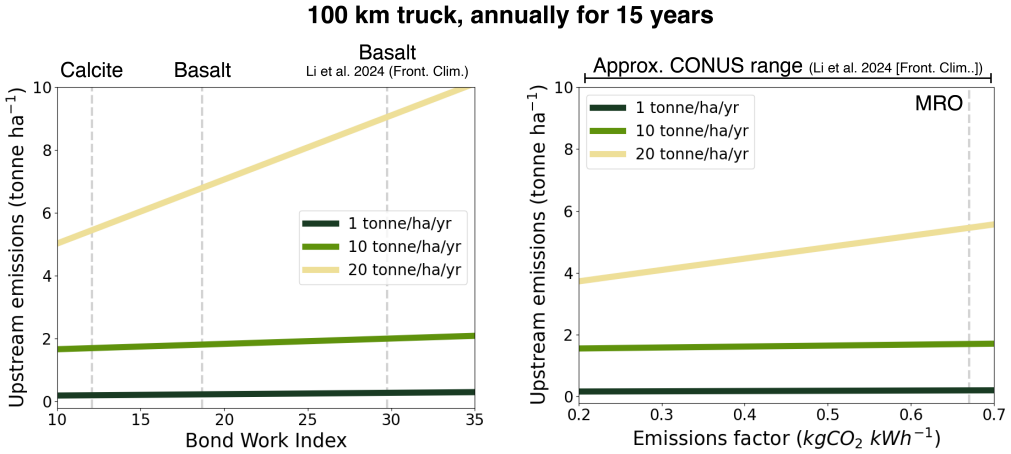

Figure S4. Upstream emissions response to varying the Bond Work Index (**A**) and the emissions factor for crushing (**B**). Emissions are cumulative over 15 years of annual, 100 km truck trips for 1, 10, and 20 tonnes of rock per hectare (dark green, green, yellow, respectively). For reference, the basalt Bond Work Index and approximate range of CONUS emissions factors estimated by Li et al. (2024) are annotated.

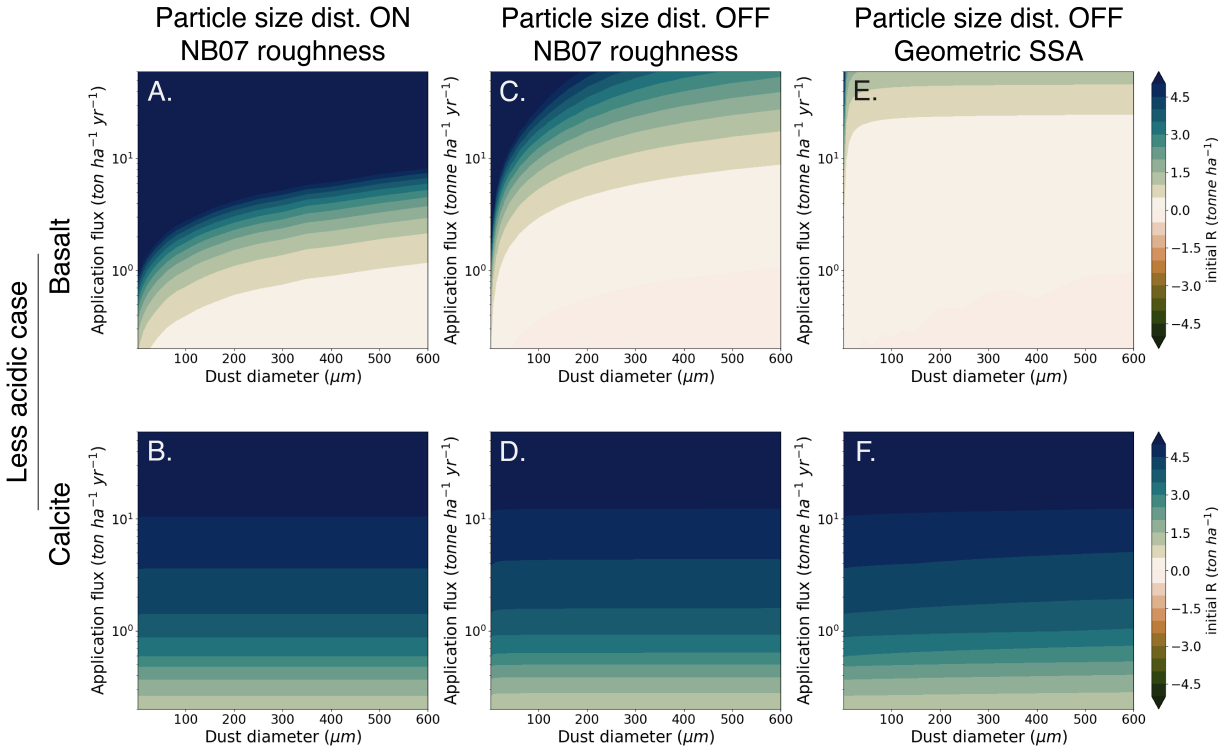

Figure S5. Basalt (top row) and calcite (bottom row) R for three weathering parameterizations (columns). (**A, B**) The case in the main text —particle size distribution tracking is on and the surface roughness is calculated following Navarre-Sitchler and Brantley (2007). (**C, D**) Particle size distribution tracking is turned off, allowing the bulk surface area to evolve with weathering while the specific surface area is constant. (**E, F**) As in (C, D) but assuming the end-member scenario of no surface roughness.

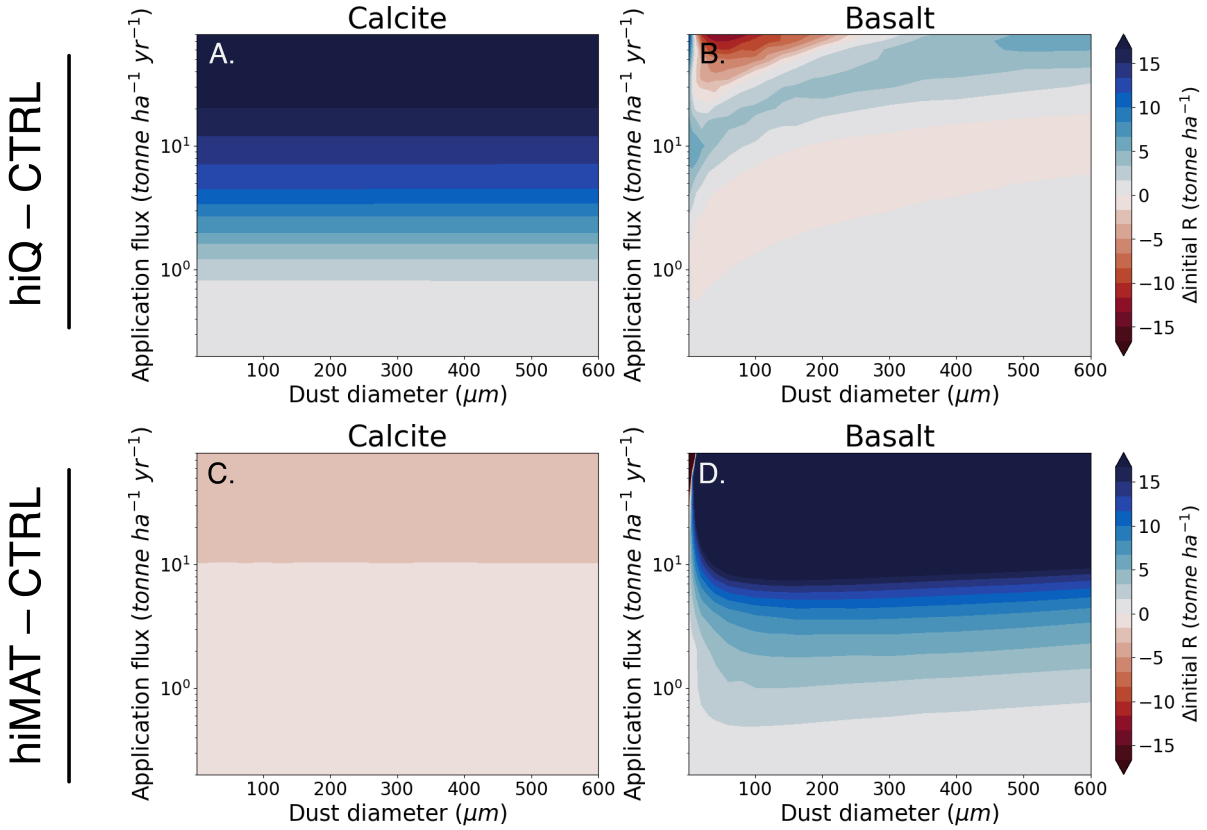

Figure S6. Effect of high soil water infiltration (Q; **A, B**) and mean annual temperature (MAT; **C, D**) on carbon removal outcomes compared to the default case presented in the main text.

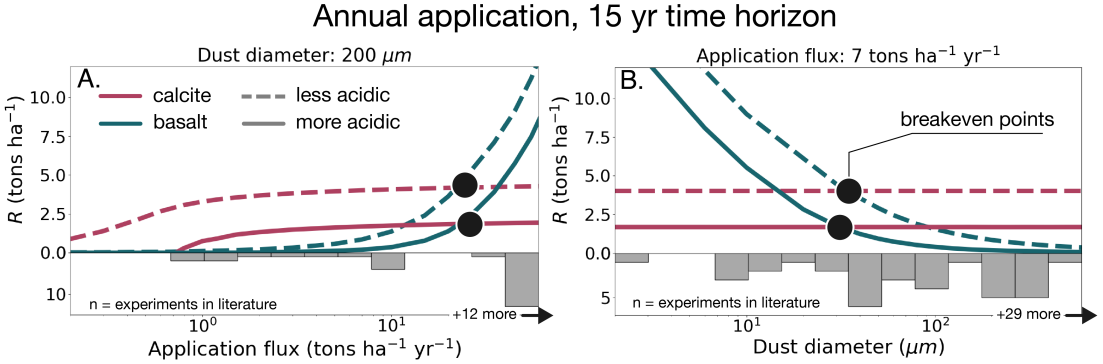

Figure S7. Basalt and calcite removal versus application flux (**A**) and dust diameter (**B**). Bars show the number of experiments in the literature for the various application flux and dust diameters as of 2023.

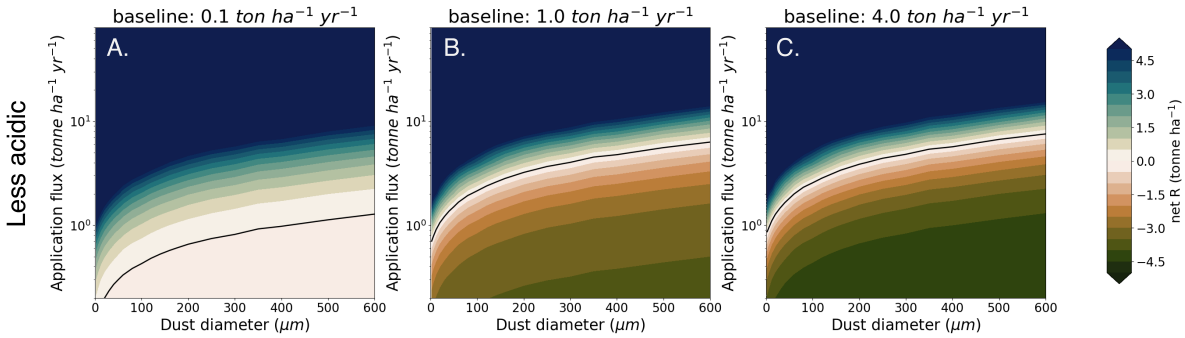

Figure S8. Basalt net removal after subtracting the effect of counterfactual liming (as in Fig. 2a of the main text) for three baseline liming scenarios: calcite applied at a rate of (**A**) 0.1 ton ha^{-1} yr^{-1}, (**B**) 1.0 ton ha^{-1} yr^{-1} (the baseline used in the main text) and (**C**) 4.0 ton ha^{-1} yr^{-1}. The particle diameter is 200 μm for each baseline scenario.

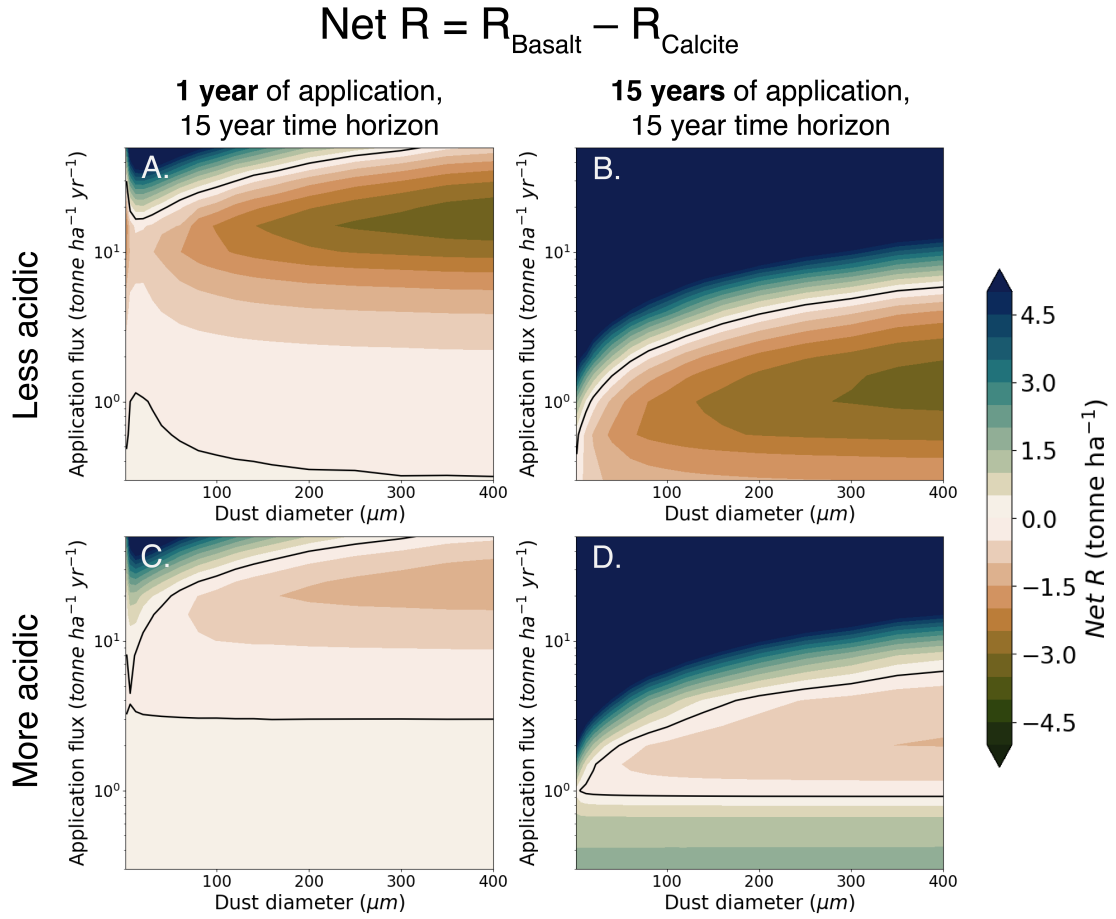

Figure S9. Comparison between basalt minus calcite net CDR for a single rock application and then 15 years of time for dissolution (**A, C**), and annual applications for 15 years (**B, D**). Unlike figures 2-5 in the main text, there is no baseline liming scenario used here. Each grid cell compares the basalt and calcite removal for the given dust diameter and application flux. Although the single application scenario gives basalt more time to weather fully, it also makes calcite less saturation-limited because less rock is spread in the 15 year interval.

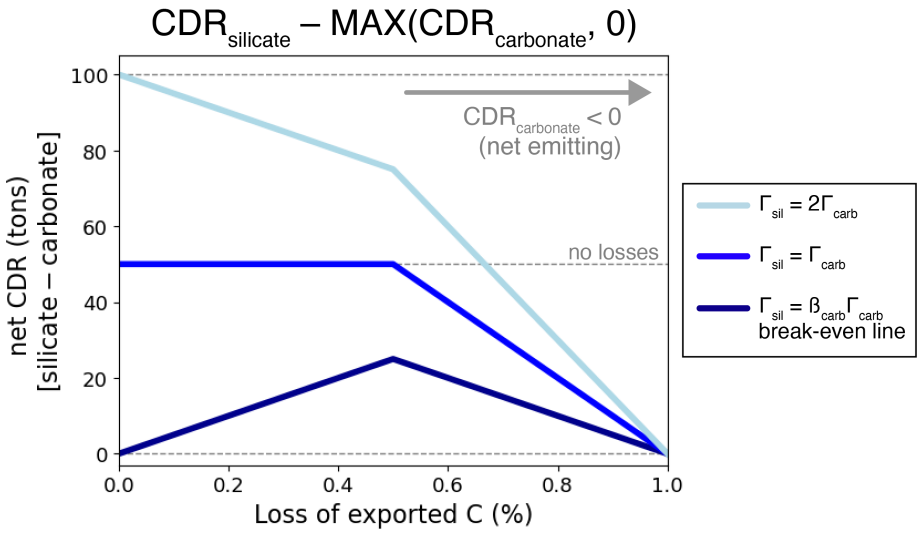

Figure S10. The effect of the loss factor (x-axis) on net CDR (y-axis) when the same loss is applied to the ERW project and counterfactual. We assume β_{carb} is the theoretical maximum of 0.5, which causes the change in slope at x=0.5.

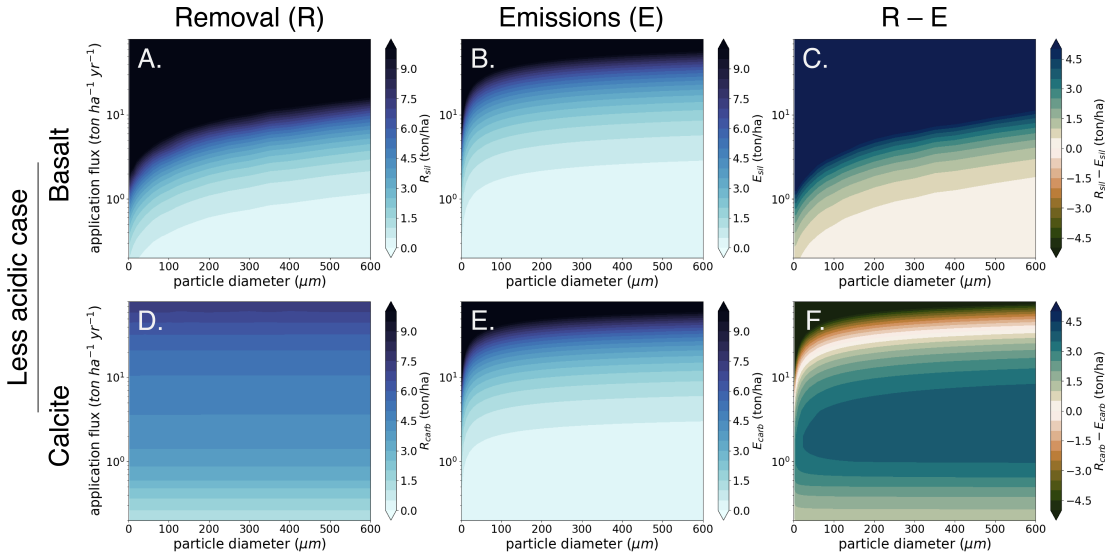

Figure S11. Initial removal (**A, D**) emissions (**B, E**) and the difference between them (**C, F**) for different particle diameters and application fluxes for basalt (**A-C**) and calcite (**D-F**). Removal flux is calculated assuming no downstream loss.

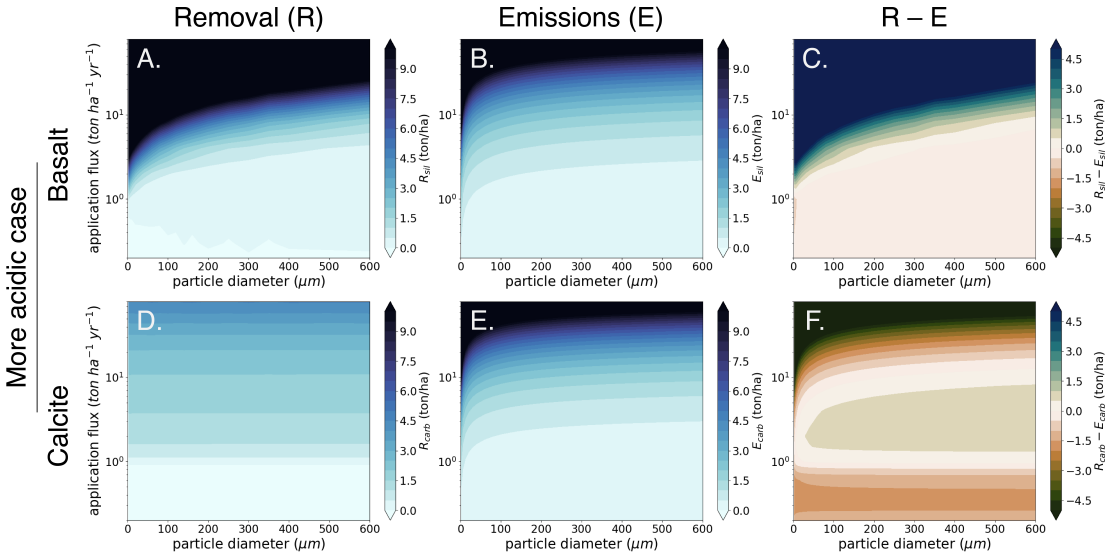

Figure S12. As figure S11 but for the more acidic case.

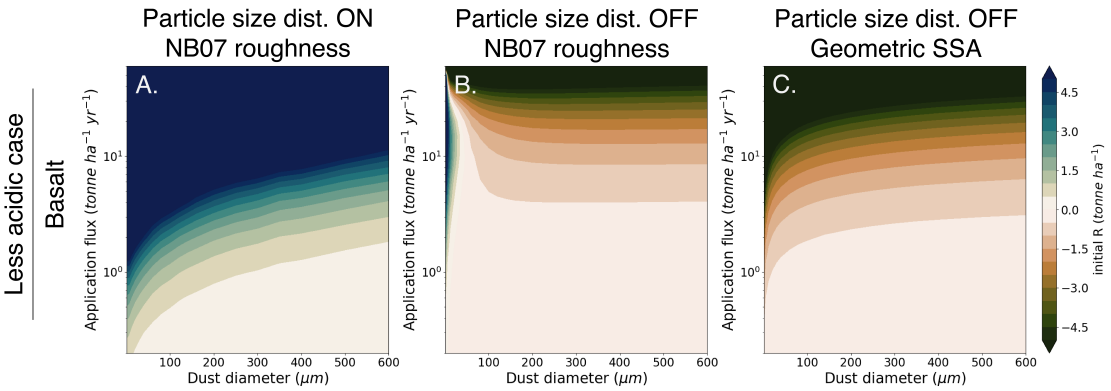

Figure S13. $R_{basalt} - E_{basalt}$ for the three surface area treatments (**A**) The case in the main text — particle size distribution tracking is on and the surface roughness is calculated following Navarre-Sitchler and Brantley (2007). (**B**) Particle size distribution tracking is turned off, such that the bulk surface area evolves with weathering while the specific surface area is constant. (**C**) As in (B) but assuming the end-member scenario of no surface roughness. Note that, unlike panel A, increasing the amount of rock applied generally increases net emissions in panels B and C.

Table S1. Variables used for SCEPTER spin-up tuning.

Variable long name	Units	Value	Variable Type
soil pH		6.06	target
organic matter	wt %	2.28	target
base saturation	%	79.02	target
soil pCO_2	log atm	-1.80	target
calcium concentration	M	1.5e-4	tuned
organic matter input	gC m^{-2} yr^{-1}	83.01	tuned
organic matter turnover time	yr	30.25	tuned
H-Na exchange coefficient	log K	4.00	tuned

Table S2. Parameters and ranges used in sensitivity analysis.

Short name	Long name	Units	Range
dustrate	Annual dust application rate	g m^{-2} s^{-1}	10-2000
dustrate_2nd	Annual fertilizer application rate	g m^{-2} s^{-1}	0-35
taudust	Duration of annual dust application	yr	0.03-0.1
dustrad	Radius of dust particles	μm	10-200
qrun	Water infiltration rate	m yr^{-1}	0.1-1.5
mat	Mean annual temperature	^{o}C	3-30
dust_mixdep	Till depth for dust mixing	m	0.05-0.4
dustrate_2nd	Annual fertilizer application rate	g m^{-2} s^{-1}	0-35
soilmoisture_surf	Soil moisture at surface	unitless	0.1-0.7

Table S3. Inputs for the upstream emissions model. Values refer to the baseline scenario and apply to both calcite and basalt amendments.

Variable name	Units	Value	Reference
p80 input	μm	1300	Zhang et al. (2023)
p80 output	μm	(feedstock diameter)	
Truck transport distance	km	0	
Barge transport distance	km	100	
Diesel barge transport distance	km	0	
Emissions factor, crushing	kg CO_2e kWh^{-1}	0.67 (MRO)	Zhang et al. (2023)
Emissions factor, truck	kg CO_2e $tonne^{-1}$ km^{-1}	0.0996	Zhang et al. (2023)
Emissions factor, barge	kg CO_2e $tonne^{-1}$ km^{-1}	0.0282	Zhang et al. (2023)
Emissions factor, barge	kg CO_2e $tonne^{-1}$ km^{-1}	0.0282	Zhang et al. (2023)
Emissions factor, diesel barge	kg CO_2e $tonne^{-1}$ km^{-1}	0.00534	Zhang et al. (2023)
Bond work index, basalt		18.67	Zhang et al. (2023)
Bond work index, calcite		12.10	Zhang et al. (2023)